ANL-6809
Physics
(TID-4500, 28th Ed.)
AEC Research and
Development Division

ARGONNE NATIONAL LABORATORY
9700 South Cass Avenue
Argonne, Illinois 60440

INTRODUCTORY FAST REACTOR PHYSICS ANALYSIS

by

David Meneghetti
Reactor Physics Division

December 1963

Operated by The University of Chicago
under
Contract W-31-109-eng-38
with the
U. S. Atomic Energy Commission

DISCLAIMER

PREFACE

Introductory Fast Reactor Physics Analysis is essentially the lecture notes of a seminar course. The lectures were presented as a part of the programs of the Scuola di Speciallizzazione in Ingegneria Nucleare of the University of Bologna and of the Centro di Calcolo (Bologna) of the Comitato Nazionale Energia Nucleare of Italy during the academic year 1962-1963 by the author during a year's visit as a consultant and lecturer. The lectures were also presented at the Comitato's Cassacia Center, near Rome, in the summer of 1963.

The lectures had the primary purpose of teaching the rudiments of fast reactor physics with emphasis on calculational analyses. The subject matter was chosen as an introduction to fast reactor analyses for persons reasonably familiar with thermal reactor physics. The intent was to present a directly practical course which at the same time would introduce sufficient subject matter to enable the student to sense the possible pitfalls in blind adherence to recipe calculations which are so tempting because of the ready availability of multigroup cross-section sets and reactor machine codes.

The sectional divisions of this report do not necessarily correspond exactly to the divisions of the lectures.

The author wishes to acknowledge the kind invitation of the Centro di Calcolo of C.N.E.N. which resulted in the preparation and presentation of the lecture series.

The author's thanks are also due to a number of Argonne colleagues who critically read the preliminary draft of this report.

TABLE OF CONTENTS

LIST OF FIGURES

LIST OF TABLES

INTRODUCTORY FAST REACTOR PHYSICS ANALYSIS

by

David Meneghetti

ABSTRACT

This report consists essentially of the lecture notes of a course in fast reactor physics analysis presented by the author. The subject matter is that of an introduction to calculational analyses of fast reactor physics for persons reasonably familiar with thermal reactor physics. Included are discussions of fast reactor characteristics, breeding, multigroup methods, cross-section definitions and evaluations, discrete ordinate transport methods, transport approximation, B_N method, asymptotic diffusion theory, equilibrium spectra, resonance effects, perturbation analysis, shape factor, lifetime, delayed-neutron fraction, reactivity-period relations, coupled systems, sodium void effect, and Doppler effect.

I. INTRODUCTION

Nuclear reactors may be classified by the distribution in energy of the neutron flux, i.e., the energy distribution of the neutrons producing fission in the fuel. Table I lists the approximate energy ranges.

Table I

ENERGY RANGE OF THE PREDOMINANT REACTOR CLASSIFICATIONS

Reactor Classification	Thermal	Intermediate	Fast
Degree of Moderation	Thermalized	Partially Thermalized	Unthermalized
Predominant Energy Range	$\lesssim$1 eV	~1 eV → ~10 keV	$\gtrsim$10 keV

The energy distribution of prompt fission neutrons have been approximated by the semi-empirical relation:[1]

$$s(E) = c\, e^{-aE} \sinh \sqrt{bE},$$

where if $a \cong 1$, and $b \cong 2$, $c \cong 0.484$, with E expressed in MeV. The spectrum is shown in Fig. 1. The constants are not, however, identical for

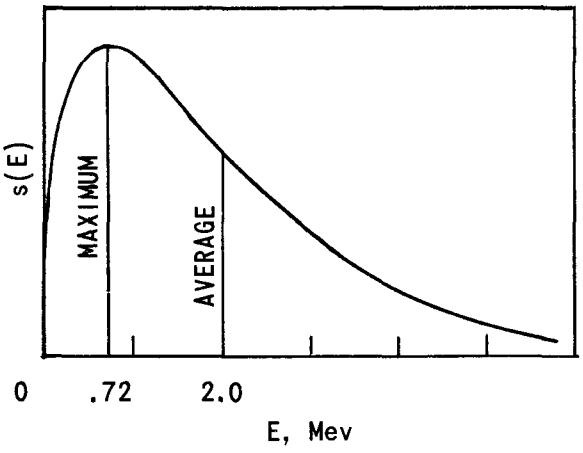

Fig. 1. Energy Spectrum of Fission Neutrons

the various fissionable materials. For example, measurements[2] gave a = 1.036, b = 2.29, and c = 0.4527 for U^{235}, and recent measurements[3] gave a = 1.05 ± 0.03, b = 2.3 ± 0.10, and c = 0.465 for U^{233}.

The energy distribution of flux in a thermal reactor is primarily due to the slowing down of the nascent fission-source distribution by elastic collision processes with the light nuclei of the moderating materials. This results in a progressive energy loss of the neutrons in the laboratory system of coordinates. A nonthermalized neutron of any energy E' furthermore has equal probability of reduction of its energy to any energy E which is between $\alpha E'$ and E', where $\alpha = (A - 1/A + 1)^2$ upon any single elastic collision event with nuclei of mass number A. This results in an increasing flux value with decreasing energy. This flux "pile-up" reaches its conclusion in the Maxwell-Boltzmann thermal distribution. The integrated magnitude of this thermal distribution in a nonleakage case depends upon the balance between the "piling-up" due to moderation and the integrated thermal absorption of the neutrons arriving at thermal energies. The absorption during slowing down is either neglected or can be considered to occur in definite energy regions, such as, for example, the epi-cadmium U^{238} capture resonances.

This transformation of the fission-source distribution, s(E), into the flux distribution can be readily seen for the case of a large (negligible leakage) hydrogen-moderated system.[1] Recalling that for hydrogen a neutron of energy E' can be changed in energy to E between E' and zero with equal likelihood by an elastic collision, one obtains the usual collision density integral balance equation:

$$\Sigma_s(E)\phi(E) = s(E) + \int_E^\infty \frac{\Sigma_s(E')\phi(E')}{E'}\, dE'.$$

The flux solution is

$$\phi(E) = \frac{s(E)}{\Sigma_s(E)} + \frac{1}{E\Sigma_s(E)} \int_E^\infty s(E')\, dE',$$

as may be verified by substitution.

At very large energies the integral is small relative to $s(E)/\Sigma_s(E)$, so that for $\Sigma_s(E) \cong$ const the flux distribution is that of the fission source As the median energy of s(E) is about 2 MeV, at $E \lesssim 1$ MeV the integral term predominates. Furthermore, when $\int_E^\infty s(E')\,dE'$ is for practical considerations constant, below ~0 1 MeV the $\phi(E)$ varies as $1/E$ if $\Sigma_s(E)$ is constant.

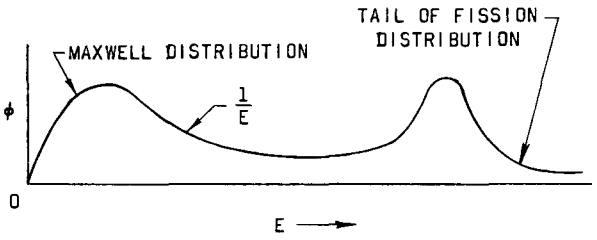

Fig. 2 General Features of Thermal System Flux (Not to Scale)

The general features of the flux distribution in a thermal system are shown in Fig 2

In contrast, the energy distribution of the flux in a nonmoderated, (i e , fast) system is largely determined by modification of the fission spectrum by inelastic scattering processes of the fast neutrons with the atoms of fuel, fertile, coolant, and structural materials (such as U^{235}, U^{238}, Na, and Fe) of fast reactors

Inelastic scattering is characterized by a threshold energy below which the interaction is zero A neutron upon being inelastically scattered to below the threshold by one or more inelastic collisions can subsequently lose additional energy only by the nearly negligible energy moderation by elastic collisions with the moderately heavy and heavy elements present or by the presence of some lighter atoms such as oxygen or carbon present as oxides or carbides of the fuel and fertile materials In any case, the slowing-down efficiency by elastic collisions is not sufficient to overcome absorptions and leakage losses during this moderation An increasing flux with decreasing energy is therefore not produced, but rather a modified and shifted fission-type distribution maximum is produced

Examples of inelastic interactions are the three lowest levels (i.e., 45, 150, and 700 keV) and numerous higher levels in U^{238}, which is frequently a principal diluent and fertile material in both core and blanket regions of fast reactors. The calculated curves in Fig. 3 indicate the general features of threshold and quasi-plateau shapes of the levels as calculated[4] by the strong-coupling statistical model.

It is to be noted that the thresholds of the lower-lying levels for the heavy fissile and fertile isotopes are low in energy relative to the bulk of the fission spectrum distribution. The low-lying levels thus affect the entire fission spectrum by shifts in energy. A neutron having energy above a given threshold will lose upon inelastic collision an increment of energy approximately equal to the value of the threshold energy if center of mass to laboratory corrections are neglected.

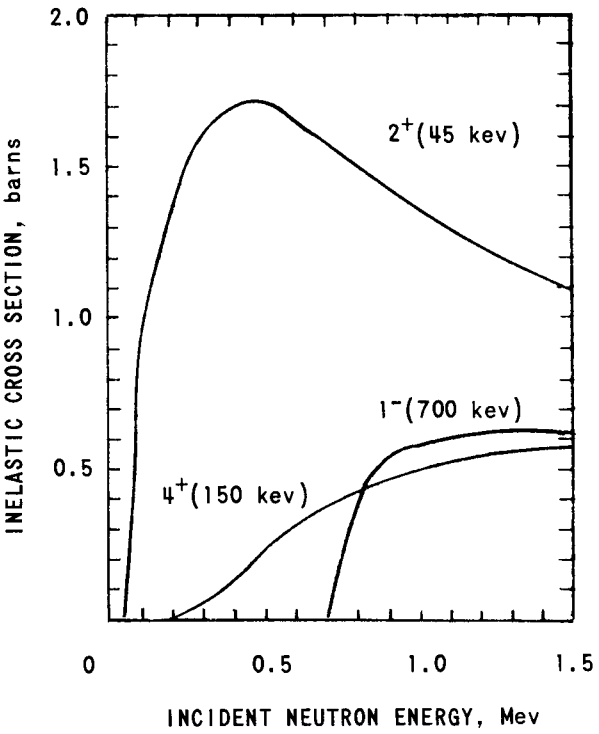

Fig. 3. Calculated Inelastic Levels in U^{238} (Ref. 4)

As a large fraction of the nascent fission spectrum lies above such threshold energies, the inelastic interactions result in incremental shifts of the entire original source distribution. Furthermore, the cross sections for absorptions cannot necessarily be neglected relative to the inelastic cross sections. Because of the variations of most cross sections with energy, a bulk treatment for absorption processes, such as the resonance escape factor of thermal reactor analyses, has not been practical. The flux distribution in energy is also quite sensitive to composition and leakage properties of the fast system.

The mode of modification of the fission spectrum by inelastic and absorption may be seen by considering an idealized simplified example. Suppose $\Sigma_{in}(E)$ a step function with threshold E_t and Σ_a a constant absorption cross section. Then the uncollided, first collision, second collision, etc., sources (see Fig. 4) are given by the expressions:

$$\text{Uncollided source} = \text{fission distribution} = s_0(E)$$

$$1^{st}\text{ collision source} = s_1(E) = \frac{\Sigma_{in}(E+E_t)}{\Sigma_{in}(E+E_t)+\Sigma_a}\, s_0(E+E_t)$$

$$2^{nd}\text{ collision source} = s_2(E) = \frac{\Sigma_{in}(E+E_t)}{\Sigma_{in}(E+E_t)+\Sigma_a}\, s_1(E+E_t)$$

$$= \left(\frac{\Sigma_{in}(E+E_t)}{\Sigma_{in}(E+E_t)+\Sigma_a}\right)\left(\frac{\Sigma_{in}(E+2E_t)}{\Sigma_{in}(E+2E_t)+\Sigma_a}\right) s_0(E+2E_t)$$

$$= \left(\frac{\Sigma_{in}(E+E_t)}{\Sigma_{in}(E+E_t)+\Sigma_a}\right)^2 s_0(E+2E_t)$$

$$n^{th}\text{ collision source} = s_n(E) = \left(\frac{\Sigma_{in}(E+E_t)}{\Sigma_{in}(E+E_t)+\Sigma_a}\right)^n s_0(E+nE_t).$$

$$\text{The flux } \phi(E) = \frac{\sum_{n=0}^{\infty} s_n(E)}{\Sigma_{in}(E)+\Sigma_a}.$$

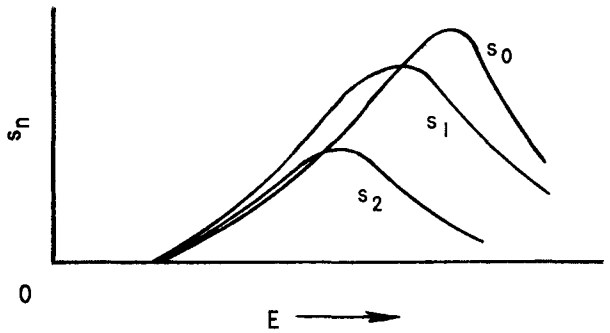

Fig. 4. General Features of the Shifted Partial Sources (Not to Scale)

The numerator is essentially the sum of shifted fission shapes with decreasing weighting. The example also indicates the important distinction between sources and fluxes. A similar example of interest would be to assume that there exists also a constant elastic-scattering cross section, Σ_s, in addition to the previous interactions, assuming that the elastic moderation however is negligible.

Elastic moderation may not, however, be generally small relative to inelastic moderation in fast reactors. On the low side of the flux maximum it can be important in determining the shape and level of the low-energy tail, where inelastic-scattering effects become small or are nonexistent.

Typical average core fluxes are those calculated[5] for the EBR-I, EBR-II and PBR. These are shown in Fig. 5. At very high energies all the distributions correspond to the high-energy fission spectrum tail shape.

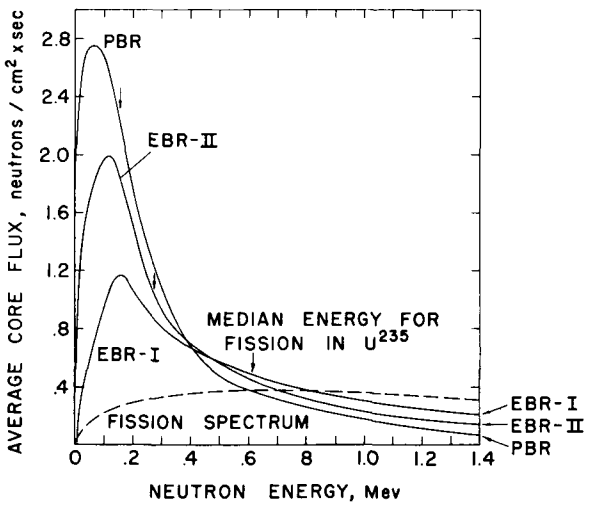

Fig. 5. Comparison of Neutron Spectra for Various Sizes of Fast Reactors (Ref. 5)

EBR-I (Experimental Breeder Reactor-I) is about a 1-MW, 6-liter, fast core fueled by highly enriched uranium fuel with stainless steel fuel cladding and NaK coolant. The breeding blanket is of natural uranium. EBR-II has instead a 50-liter core volume and is fueled by about 50% enriched uranium fuel. The PBR (Power Breeder Reactor) flux is representative of a 800-liter core, fueled by 15 to 20% enriched uranium, or Pu-U^{238}, fuel and having a power of greater than 600 MW of heat. Coolants occupy about 50% of the core volumes. It has been noted[5] that although the energy position of the maxima are not much displaced relative to one another, the median energies, however, are much different.

Another characteristic of fast systems is the large amounts of fuel required, i.e., critical mass, relative to a thermal system of, for example, the same core volume. This results primarily because of the relatively small values of cross sections in the high-energy region of fast reactors

in contrast with the magnitudes of thermal cross sections. For example, the U^{235} fission and capture cross sections are hundreds of times smaller than in the thermal-energy region. Approximate order-of-magnitude values for U^{235} are given in Table II.

Table II

APPROXIMATE CROSS SECTIONS OF U^{235} IN THERMAL AND FAST SYSTEMS

	Thermal (2200 m/sec)	Fast[8]
σ_f, b	582[6]	≈ 1.4
σ_c, b	101[6]	≈ 0.25
σ_{tr}, b	698 [$\sigma_s \approx 15$ b[7]]	≈ 6.8

Similar orders of magnitudes exist for the fissionable U^{233} and Pu^{239} species as well as for the usual fertile and diluent materials. The values for the fast systems are greatly dependent upon the neutron flux spectrum distribution.

This consideration emphasizes the importance of reducing core volume by increasing the fuel density.

To a large extent this is possible because no volume is required for moderator material. Further reduction of core volume is generally limited in power-producing systems by the large coolant volumes required to insure removal of the heat consistent with the total power and the temperature limitations of the materials.

Thus, the minimum practical core size is fixed by the amount of power per unit of core volume that can be handled by the coolant volume and coolant flow. The overall results are that a fast reactor has a higher power density per unit core volume than a liquid-cooled thermal system of the same total power.

II. BREEDING

In view of the larger critical masses and power densities per unit volume of a fast reactor relative to a thermal reactor, one might ask why consider a fast reactor except for special cases where smaller volume requirements are necessary. The answer, of course, is the possibility of existence of effective breeding ratios sufficiently larger than unity so that in practice the entire conversion of the natural supply of otherwise non-fissionable fertile materials may be efficiently converted to fissionable materials and thereby become available for power production.

Fertile materials such as U^{238} or Th^{232} are placed in the reflector blankets of fast reactors for breeding purposes. Generally, fertile material is also present as a core diluent for core breeding.

Consider the conversion of the nonthermally fissionable U^{238} isotope into the thermally fissionable plutonium isotopes of odd atomic mass number. The reaction chain for this case is reproduced in Fig. 6.(8)

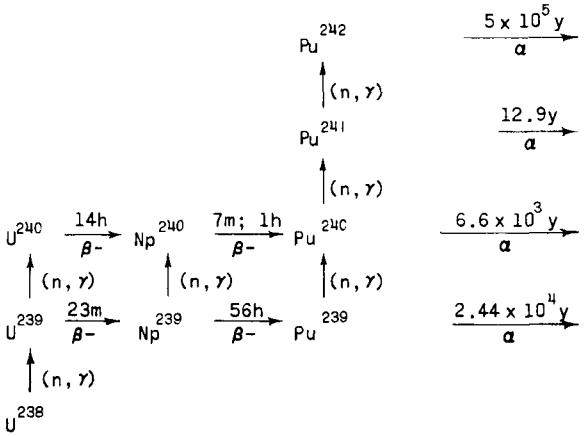

Fig. 6. Nuclear Reactions under Neutron Irradiation of U^{238} (Ref. 8)

Irradiated U^{238} fertile material thus contains a mixture of higher plutonium isotopes. The isotopic composition of the contained plutonium will depend upon the particular reactor system, because of the spectral dependence of the neutron cross sections in the build-up chain, and upon the previous irradiation history of the fertile material. Recycle, of the plutonium isotopes in a reactor will change the isotopic concentrations. An equilibrium condition will ultimately be approached which is a function of fuel cycle, core design, and feed material.

For example, the plutonium isotopic composition (in a/o): Pu^{239}, 74.7%; Pu^{240}, 10.2%; Pu^{241}, 12.4%; and Pu^{242}, 2.7%, is reported(9) to correspond to a recycle plutonium extracted from a thermal reactor fueled with enriched uranium oxide, such as the "Yankee" reactor. For comparison, a reported(9) case of extreme recycling is:

Pu^{239}, 40%; Pu^{240}, 10%; Pu^{241}, 25%; Pu^{242}, 25%.

Plutonium feed material containing also the higher isotopes is referred to as "dirty." It is interesting to note that in a calculational

study[9] the so-called "dirty" plutonium used as fuel in a fast reactor resulted in larger values of the breeding ratio.

The analogous Th^{232} build-up chain is shown in Fig. 7.[8]

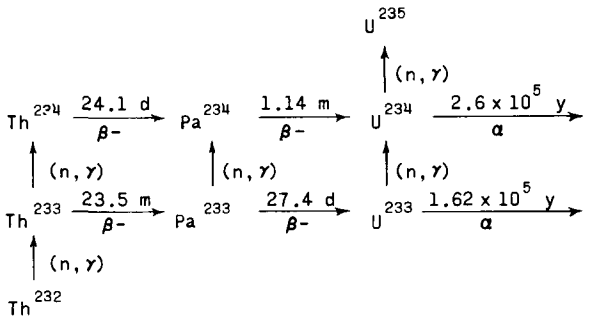

Fig. 7
Nuclear Reactions under Neutron Irradiation of Th^{232} (Ref. 8)

For present discussion, the breeding ratio will be taken as

$$BR \equiv \frac{\text{Quantity of fresh, thermally fissile fuel produced}}{\text{Quantity of primary thermally fissile fuel destroyed}},$$

and the distinction between conversion and breeding will not be adhered to. The various definitions of breeding ratio are discussed in Ref. 10.

Considering that the amount of fertile material is much greater than the amount of fissile materials in the Earth's crust, then in order to insure complete conversion of all the fertile U^{238} and Th^{232}, a breeding ratio of one or greater must be obtained. If $(BR) < 1$, then by continued burning up of previously bred fuel one would obtain but a limited utilization of the Earth's resources. An atom of primary fissile material would result in (BR) new fissile atoms. The latter when consumed would result in $(BR)^2$ new fissile atoms, and so forth. The total atoms of fissile fuel ultimately used would be

$$1 + (BR) + (BR)^2 + \ldots = \frac{1}{1 - (BR)}.$$

For each original fissile atom consumed, only

$$\frac{1}{1 - (BR)} - 1 = \frac{BR}{1 - BR}$$

atoms of fertile would have been transformed to fissile atoms.

For each atom of natural uranium, only about 0.007 atom are the fissile U^{235} species. Theoretically for complete burn-up, then,

$$\frac{1}{1 - (BR)} - 1 = \frac{1 - 0.007}{0.007} = \frac{1}{0.007} - 1$$

from which

$$BR \geq 0.993 \approx 1.$$

A measure of the effectiveness of a given fissile material to contribute its excess fission neutrons for fertile capture is $\eta - 1$ of the fissile atom:

$$\eta - 1 = \frac{\nu - 1}{1 + \alpha}$$

where

$$\alpha = \sigma_c/\sigma_f.$$

A larger value of $\eta - 1$ is obtained with larger ν and/or smaller α. Both ν and α are dependent upon the energy of the incident neutron. It turns out that ν increases with energy. For example, for U^{235},(11)

$$\nu(E) = 2.43 + 0.115\, E_n \text{ up to } 1.5 \text{ MeV};$$

and

$$\nu(E) = 2.406 + 0.138\, E_n \text{ from } 1.5 \text{ MeV to } 15 \text{ MeV}.$$

In addition, although both σ_c and σ_f decrease with increasing energy, the ratio of σ_c/σ_f over the spectrum of a fast reactor is smaller than that over a thermal reactor.

Some approximate values of $\eta - 1$ are listed in Table III.

Table III

VALUES OF $\eta - 1$ FOR FISSILE MATERIALS IN THERMAL AND FAST SYSTEMS

	Thermal (2200 m/s)	Fast(12)
U^{235}	1.07(6)	~1.18
Pu^{239}	1.00(6)	~1.74
U^{233}	1.29(6)	~1.42

The values for the fast spectrum are especially sensitive to the spectrum.

If allowance is made for possible processing losses, leakages, and parasitic absorptions, only the U^{233}-fueled thermal system would appear attractive. The values of the fast $(\eta - 1)$ should in addition be augmented by the ever-present fission neutrons due to fast fission in U^{238} and to a smaller extent in Th^{232}. From the cross section versus energy measurements,[13] the shape for the fast fission process is roughly sketched in Fig. 8. The fast spectrum is sufficiently high in energy that an appreciable portion of the flux is above the fast fission threshold energies of the fertile materials. This has been reported to increase the BR > 2 for a fast Pu^{239}-U^{238} system.[15] In practice a ratio ~1.7 with Pu^{239} fuel and ~1.2 with U^{235} fuel may be expected.[12]

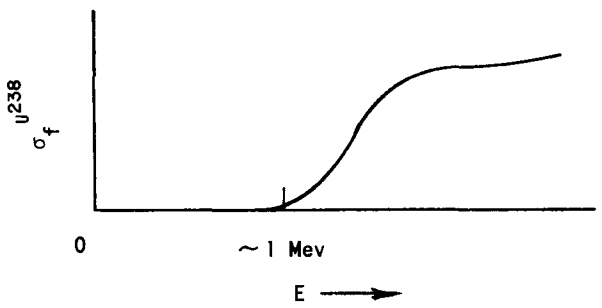

Fig. 8. General Features of Fission Cross Section of U^{238} (Not to Scale)

Theoretically, neglecting losses, if BR = 1, the number of fissionable nuclei existing at any time equals the number of original fissile nuclei so that the total available fissile material at any time does not increase. For a breeding gain G = (BR) - 1, the breeding ratio must be > 1. An important quantity in this regard is the doubling time, D.T., which is related to the gain:

$$\text{D.T.}_{\text{days}} = \frac{\text{critical mass in grams}}{\text{grams fissile gained per day}} = \frac{\text{critical mass in grams}}{(\text{G})\,(\text{grams fissile consumed per day})}.$$

The fissile burn-up rate is related to the power and the capture-to-fission ratio:

$$(\text{grams fissile consumed/day}) = \frac{P_{\text{watts}}}{10^6}(1+\alpha),$$

from which

$$\text{D.T.}_{\text{days}} = \frac{10^6}{G p_{\text{watts}}\,(1+\alpha)},$$

where p is the specific power in watts.[14] A large breeding ratio and a large power density per unit mass of fissile material lead to small doubling times. For completeness, the time for processing and extracting the new fuel, the amount of fuel held external to the reactor in reprocessing plants, shutdown time, and the fraction of the power due to fast fissions in fertile material must also be considered.[14,15] The doubling time may then be expressed as

$$\text{D.T.}_{\text{days}} = \frac{10^6}{GI(1-F)p(1+\alpha)L},$$

where I is the ratio of reactor critical mass to total fuel in reactor and hold-up outside of reactor, L is the fraction of time the reactor is in operation, and F is the fraction of power due to fertile fast fissions. The large fertile fast fission of fast reactors is conducive to lowering of doubling time.

Another quantity of interest is the burnup. It is usually a fraction equivalent to a couple of percent in fast systems. It may be defined as

$$\text{Burnup} = \frac{\text{atoms fissioned in the "fuel"}}{\text{original atoms of fissile, fertile, and diluent materials in the "fuel"}}.$$

The general or central problems of fast reactors arise from the need for high power density per unit mass of fissile material. This results in the need for high temperatures of operation, high heat-transfer rates from fuel to coolant, and high burnup in order to minimize the high fuel inventory holdup during reprocessing. High operating temperatures require thin or finely divided fuel to obtain better heat transfer. The Fermi Fast Breeder Reactor, for example, has fuel pins 0.158 in. in diameter and about 30 in. long.(16)

Coolants are required which cause negligible elastic moderation, have good high-temperature heat transfer, and do not attack the cladding materials of the fuels. The eutectic mixture NaK and the element sodium have been found particularly good. In addition, they have relatively low melting and high boiling temperatures.

Technological problems in fast reactors are discussed, for example, in the text of Palmer and Platt.(15)

To reduce the costs of inventory, reprocessing and refabrication of fuel, the problem of achieving high burnup is paramount. The high temperatures, however, produce, through the increased pressure arising from the internal accumulation of fission product gases, a swelling of fuel. The importance of high burnup in fast reactors can be appreciated if one considers that the density of fuel is greater by a factor of ten in a fast fuel than in a thermal fuel element.

Because of radiation damage, removal of fuel elements may become necessary when a couple of percent of fissionable and nonfissionable atoms have burned up. At this time an amount of fuel about equal to the initial fissile mass of a thermal reactor would be consumed, whereas this represents only of the order of 10% of the fuel in the fast reactor. Thus of the

order of 10 reprocessings would be required for complete use of the fuel.[17] Fuel burnup in a thermal system is more limited by the available excess reactivity to overcome fission product poisons. In a fast system, because of the small cross sections of the poisons at high energies, the burnup is more limited by radiation damage.

Last, but perhaps not the least, is the question of the relative safety merits of fast and thermal systems. This will be discussed in more detail later. Suffice it to say that the potential greater hazards in fast systems are usually related to the shorter prompt-neutron lifetime, the possible loss of coolant (with possible attendant increase in reactivity due to spectral shift effects), and/or radiation heating of the fuel elements so as to possibly produce a super-critical meltdown configuration. There exists also the possibility of resonance coupling of reactivity and power in some cases.[18]

III. MULTIGROUP METHOD

In the energy range of fast reactor spectra the variations of cross sections with energy are sufficiently large that bulk treatment of large energy regions in correspondence to, say, a four-factor formula has not as yet been successful in practice. Methods of multigroup solutions of transport or diffusion equations are used instead. As the dimensions of fast reactor regions are not large relative to the mean free paths, i.e., a distance of a mean free path is an appreciable fraction of the regional dimension, transport solutions are required for the smaller fast systems and generally also for precise calculations on the larger fast systems.

Although not basically as accurate, the diffusion theory approximation is much used. Indeed, because of lack of cross-section information the use of diffusion theory for all but very precise comparisons is usually adequate except for the small systems.

Simplified two-group diffusion equations with transfer coefficients coupling the groups are, for the case of thermal systems,[19]

$$D_1\nabla^2\phi_1 - \Sigma_{a_1}\phi_1 + S_1 = 0;$$

$$D_2\nabla^2\phi_2 - \Sigma_{a_2}\phi_2 + S_2 = 0.$$

The group sources are

$$S_1 = \nu\Sigma_{f_2}\phi_2$$

and

$$S_2 = \Sigma_{a_1}\phi_1.$$

The thermal flux (ϕ_2) produces the fission neutron sources of group one. The fast flux group (ϕ_1) produces the neutron sources in the thermal group by moderation transfer of neutrons, i.e., $\Sigma_{a_1} \equiv \Sigma_{1\to 2}$. Furthermore, the relations between transfer coefficients and parameters entering the four-factor formula through k_∞, L^2, and τ are

$$\Sigma_{a_1} = \frac{D_1}{\tau}; \qquad \Sigma_{a_2} = \frac{D_2}{L^2}; \qquad \nu\Sigma_{f_2} = k_\infty\Sigma_{a_2} = k_\infty\frac{D_2}{L^2}.$$

In the case, for example, of a two-group analysis of fast systems, the lower energy of the lower group need not be zero. Below some lower energy limit the contribution to, for example, the reactivity is negligible. Considerations of both capture and fission as well as the fractional distribution of the fission spectrum is necessary. The two group sources would then be

$$S_1 = \chi_1 (\nu\Sigma_f)_1 \phi_1 + \chi_1 (\nu\Sigma_f)_2 \phi_2$$

and

$$S_2 = \Sigma_{1\to 2} \phi_1 + \chi_2 (\nu\Sigma_f)_2 \phi_1 + \chi_2 (\nu\Sigma_f)_2 \phi_2,$$

where χ_1 and χ_2 are the fractions of the fission spectrum,

$$\Sigma_{a_1} = \Sigma_{c_1} + \Sigma_{f_1} + \Sigma_{1\to 2},$$

and

$$\Sigma_{a_2} = \Sigma_{c_2} + \Sigma_{f_2}.$$

The extension to J groups then follows. For each group j, the equation is of the form

$$D_j\nabla^2\phi_j - \Sigma_{a_j}\phi_j + S_j = 0,$$

where

$$S_j = \sum_{i=1}^{j-1} \Sigma_{i\to j} \phi_i + \chi_j \sum_{i=1}^{J} (\nu\Sigma_f)_i \phi_i + S_{0_j}.$$

Here S_{0_j} is zero except in the case of applied sources. Also,

$$\Sigma_{a_j} = \Sigma_{c_j} + \Sigma_{f_j} + \sum_{k=j+1}^{J} \Sigma_{j\to k}.$$

A particularly simple solution, amenable also for hand computation, is possible even with many groups in the case of a bare, homogeneous system if it be assumed that extrapolation distances are equal in all groups.(5) By assuming that all groups satisfy the equation

$$\nabla^2\phi_j + B^2\phi_j = 0,$$

one may, by an iterative solution method, determine the group flux values ϕ_j, and the value of B^2 for which neutron production equals neutron absorption plus leakage, i.e., $k_{eff} = 1$.

Taking a group at a time and assuming an initial guess for B^2, we find

$$-D_1B^2\phi_1 - \Sigma_{a_1}\phi_1 + S_1 = 0,$$

so that

$$\phi_1 = S_1/(\Sigma_{a_1} + D_1 B^2);$$

similarly,

$$\phi_2 = S_2/(\Sigma_{a_2} + D_2 B^2);$$
$$\vdots$$
$$\phi_J = S_J/(\Sigma_{a_J} + D_J B^2).$$

The group sources are given by

$$S_j = \chi_j \sum_{k=1}^{J} (\nu\Sigma_f)_k \phi_k + \sum_{k=1}^{j-1} \Sigma_{k\to j} \phi_k = \chi_j + \sum_{k=1}^{j-1} \Sigma_{k\to j} \phi_k,$$

from which

$$k_{eff} = \frac{\sum_{j=1}^{J} (\nu\Sigma_f)_j \phi_j}{\sum_{j=1}^{J} \chi_j} = \sum_{j=1}^{J} (\nu\Sigma_f)_j \phi_j.$$

The denominator is the initially assumed fission source distribution whose value is taken as unity:

$$\sum_{1}^{J} \chi_j = 1.$$

Another B^2 value is then chosen and the procedure repeated until k_{eff} is sufficiently close to unity. The material buckling, B^2, may then be related to the geometrical buckling of a bare homogeneous system having extrapolated dimensions. The relative magnitudes of the fluxes in each energy group are also obtained.

In the middle of the central region of a multiregion reactor system the spectrum should be close to that of the bare core.

As a simple example of the procedure and also to obtain a feel for group cross sections, consider the following two-group parameters to apply to the simple composition: 10% U^{235} and 70% U^{238}.

Assume atomic densities 0.048 in units of 10^{24} and microscopic cross sections given in Table IV. The homogenized macroscopic cross sections are listed in Table V. If B^2 is guessed to be 0.005 cm^{-2}, the fluxes are calculated to be $\phi_I = 5.07$ and $\phi_{II} = 39.8$. The k_{eff} value is 1.005. For a value closer to unity, assume a somewhat larger B^2 value and repeat the procedure.

Table IV

TWO-GROUP FAST CROSS SECTIONS
(IN BARNS) FOR U^{235} AND U^{238}

		U^{235}	U^{238}
Group I 1.35 MeV → 10 MeV $\chi_1 = 0.574$	$\nu\sigma_{f_1}$	3.44	1.48
	$3\sigma_{tr_1}$	14	14
	σ_{a_1}	2.8	2.7
	$\sigma_{I\rightarrow II}$	1.4	2.1
Group II 9.12 keV → 1.35 MeV $\chi_2 = 0.426$	$\nu\sigma_{f_2}$	3.50	0
	$3\sigma_{tr_2}$	18	21
	σ_{a_2}	1.7	0.18

Table V

HOMOGENIZED TWO-GROUP
FAST CROSS SECTIONS

	Group I (cm^{-1})	Group II (cm^{-1})
$\nu\Sigma_{f_1}$	0.0662	0.0168
$3\Sigma_{tr_1}$	0.538	0.792
Σ_{a_1}	0.104	0.0142
$\Sigma_{1\rightarrow 2}$	0.077	0

For the flux solutions in the various regions of a multigroup-multiregion case, iterative energy and spatial methods of solution are used.[20] Assume a fission source distribution, $S_f^0(\vec{r})$; and $\chi_j S_f^0(\vec{r})$ as the distribution in energy group j. Then,

$$D_1(\vec{r})\nabla^2\phi_1(\vec{r}) - \Sigma_{a_1}(\vec{r})\phi_1(\vec{r}) + \chi_1 S_f^0(\vec{r}) = 0$$

is solved for $\phi_1(\vec{r})$. The approximate group-2 source, calculated by

$$S_2(\vec{r}) = \Sigma_{1\to 2}(\vec{r})\,\phi_1(\vec{r}) + \chi_2 S_f^0(\vec{r}),$$

is employed analogously to obtain $\phi_2(\vec{r})$. Similarly, the group-3 source approximation is

$$S_3(\vec{r}) = \Sigma_{1\to 3}(\vec{r})\,\phi_1(\vec{r}) + \Sigma_{2\to 3}(\vec{r})\,\phi_2(\vec{r}) + \chi_3 S_f^0(r),$$

etc.

By means of the calculated $\phi_j(\vec{r})$, the derived fission source distribution

$$S_f^1(\vec{r}) = \sum_{j=1}^{J} \nu\Sigma_f(\vec{r})_j\phi_j(\vec{r})$$

may be compared with the initial, or previous, iteration, $S_f^0(\vec{r})$. If $S_f^1(\vec{r}) = S_f^0(r)$ the system is critical. If

$$S_f^1(\vec{r})/S_f^0(\vec{r}) = \text{constant} \neq 1,$$

the problem is solved and the system has $k_{eff} = S_f^1(\vec{r})/S_f^0(\vec{r})$. For further adjustment to obtain criticality, changes in regional dimensions and/or compositions are required and the procedure is repeated.

IV. DIFFERENCE EQUATIONS

Numerical solutions of the multiregion-multigroup equations by digital computers necessitate transformation of the spatially dependent, coupled multigroup differential equations to a system of coupled difference equations.[21]

For any energy group j of a given homogeneous region, the differential equation is

$$D_j \nabla^2 \phi_j(\vec{r}) - \Sigma_{a_j} \phi_j(\vec{r}) + S_j(\vec{r}) = 0.$$

In spherical geometry one obtains

$$\frac{d^2\psi_j(r)}{dr^2} - \frac{\Sigma_{a_j}\psi_j(r)}{D_j} + \frac{rS_j(r)}{D_j} = 0,$$

where $\psi(r) = \phi(r)/r$. The equation of each group is of the form

$$\frac{d^2\psi(r)}{dr^2} - \kappa^2\psi(r) + r\mathcal{S}(r) = 0.$$

Consider a spherical system of two concentric regions. Define

$$\psi_n \equiv \psi(r_n) \text{ and } \mathcal{S}_n \equiv \mathcal{S}(r_n),$$

where r_n is the value of r at the n'th mesh point position, r_0 being the center of the system. Assume constant mesh separation Δ_1 and Δ_2 in the respective regions.

A difference expression for the Laplacian at a position r_n within a region is

$$\frac{d^2\psi}{dr^2} = \frac{1}{\Delta}\left[\left(\frac{\psi_{n+1} - \psi_n}{\Delta}\right) - \left(\frac{\psi_n - \psi_{n-1}}{\Delta}\right)\right] = \frac{\psi_{n+1} - 2\psi_n + \psi_{n-1}}{\Delta^2}.$$

The quantity in the bracket is seen to be just the difference in derivatives of ψ between the pairs of mesh points, r_{n-1} to r_n and r_n to r_{n+1}. The difference equation of a given group and region is then of the form

$$\psi_{n+1} - (\kappa\Delta^2 + 2)\psi_n + \psi_{n-1} + r_n\Delta^2\mathcal{S}_n = 0.$$

A mode of difference solution[20] for the spatial dependence, amenable to hand calculation, may be illustrated by considering a one-energy

group, one-region example with a given spatially applied source distribution. The previous difference equation may be rewritten in the form

$$\psi_{n+1} - k\psi_n + \psi_{n-1} + T_n = 0.$$

Given the source-dependent values of T_n, with $n = 0,\ldots,N$, the problem is to determine ψ_n for $n = 0,\ldots,N$. Further simplification of form for calculational ease is possible. Let A_n be the solution of the homogeneous equation

$$\psi_{n+1} - k\psi_n + \psi_{n-1} = 0.$$

Then

$$A_n(\psi_{n+1} - k\psi_n + \psi_{n-1} + T_n) = 0$$

and

$$\psi_n(A_{n+1} - kA_n + A_{n-1}) = 0.$$

The difference of these two expressions,

$$(\psi_n A_{n+1} - A_n \psi_{n+1}) + (A_{n-1}\psi_n - A_n\psi_{n-1}) - A_n T_n = 0,$$

may then be expressed as

$$P_n - P_{n-1} = A_n T_n,$$

where

$$P_n = A_{n+1}\psi_n - A_n \psi_{n+1}.$$

Assuming, then, a homogeneous slab, with zero-flux boundary conditions and applied spatial source distribution, the problem is to find ψ_n subject to the conditions $\psi_0 = \psi_N = 0$.

Using the homogeneous equation

$$A_{n+1} = kA_n - A_{n-1}$$

with $A_0 = 0$ by the boundary condition and with $A_1 = 1$ for ease, as the value of latter quantity divides out in final answer for ψ_n, calculate outwardly the A_n values from $A_2,\ldots A_n$.

Next, using the equation $P_n - P_{n-1} = A_n T_n$ with conditions $P_0 = 0$ by the boundary condition, obtain $P_1,\ldots,P_n$ by working outward.

Finally, by employing the definition of P_n in the form

$$\psi_n = \frac{P_n + A_n \psi_{n+1}}{A_{n+1}}$$

and applying the outer boundary condition $\psi_N = 0$, work inward to obtain

$$\psi_{N-1}, \psi_{N-2}, \cdots, \psi_1.$$

For the case of a one-group multiregion problem the analysis proceeds similarly with, however, application of interface boundary conditions of continuity of flux and current. For cases of source distributions which are flux induced by, for example, the fission reaction, iterations of the spatial flux and source distributions are carried out until shape convergence is obtained.

The difference-expression formula for the current requires some consideration. The difference expressions for Laplacian and gradient together with the formula used in the volume integrations over mesh points must satisfy the divergence theorem:

$$\int_V \bar{\nabla} \cdot \bar{\nabla} \phi \, dV = \int_S \bar{n} \cdot \bar{\nabla} \phi \, dS.$$

In this manner there is assured that for any volume region and energy group the neutron balance

$$J_{out} = J_{in} - \Sigma_a \int \phi \, dV + \int S dV$$

is satisfied. Naturally this, of course, does not mean that there are then no errors in the difference formulations, but only that the neutron balance is internally consistent. Having thus decided upon an expression for the Laplacian $(\nabla^2 \phi)_n$, at a mesh point, it may be easily shown by use of the divergence theorem that if, for example, the trapezoidal integration formula

$$\int_{r_A}^{r_B} f_n(r_n) \, dr_n \cong \frac{f_A \Delta}{2} + \sum_{A+1}^{B-1} f_n \Delta + \frac{f_B \Delta}{2}$$

is employed, the difference expression for the gradient at a mesh point must be

$$(\nabla \phi)_n = \left(\frac{\phi_{n+1} - \phi_{n-1}}{2\Delta} \right)$$

for the case of slab geometry, where Δ is the mesh point separation. For the case of spherical geometry the gradient difference expression becomes

$$\left(\frac{d\phi}{dr}\right)_n = \left(\frac{\psi_{n+1} - \psi_{n-1}}{r_n\, 2\Delta}\right) - \frac{\psi_n}{r_n^2}.$$

The latter form may be seen directly by neglect of $(\Delta)^2$ terms in the development given in Ref. 20.

V. GROUP PARAMETERS AND CROSS-SECTION DEFINITIONS

In the discussions of the multigroup method, nothing has yet been said about procedures for evaluation of the multigroup cross-section parameters, i.e., given the energy dependence of the various microscopic cross-section interactions, what is a possible procedure for obtaining the homogenized (macroscopic) group cross section for a given energy interval.

Possible homogenized parameters for a diffusion theory calculation are

D_j,	group diffusion parameter
$(\nu\Sigma_f)_j$,	effective group value of ν and the fission cross sections
Σ_{c_j}	group capture cross section
Σ_{f_j},	group fission cross section
$\Sigma_{el_{j\to k}}$,	elastic transfer cross section from group j to k
$\Sigma_{in_{j\to k}}$,	inelastic transfer cross section from group j to k.

The group total cross section, which is not generally used directly in diffusion theory calculations, is

$$\Sigma_{total_j} = \Sigma_{c_j} + \Sigma_{f_j} + \Sigma_{el_j} + \Sigma_{in_j},$$

where Σ_{el_j} and Σ_{in_j} include all elastic and inelastic scattering events occurring in group j. The group scattering cross sections are related to the transfer cross sections by the expressions

$$\Sigma_{el_j} = \Sigma_{el_{j\to j}} + \Sigma_{el_{j\to j+1}} + \Sigma_{el_{j\to j+2}} + \text{etc.}$$

and

$$\Sigma_{in_j} = \Sigma_{in_{j\to j}} + \Sigma_{in_{j\to j+1}} + \Sigma_{in_{j\to j+2}} + \text{etc.},$$

where the $j\to j$ terms represent scattering which remain within the energy interval of the group.

Assuming that a priori knowledge of $\phi(E)$ within an energy group is known, then, for example,

$$\Sigma_{c_j} = \frac{\int_{E_{j_{lower}}}^{E_{j_{upper}}} \Sigma_c(E)\,\phi(E)\,dE}{\int_{E_{j_{lower}}}^{E_{j_{upper}}} \phi(E)\,dE},$$

where

$$\Sigma_c(E) = \sum_{m_{materials}} N^m\,\sigma_c^m(E).$$

Here N^m is the atomic density (units of 10^{24} atoms per cm^3) of material m present in the mixture, and $\sigma_c(E)$ is the microscopic cross section in barns. The summation process is referred to as homogenization. With such an averaging formula, the averaging can also precede the homogenization summation.

It is seen that

$$\Sigma_{c_j} = \frac{\int_{E_{j_{lower}}}^{E_{j_{upper}}} \left(\sum_m N^m\,\sigma_c^m(E)\right)\phi(E)\,dE}{\int_{E_{j_{lower}}}^{E_{j_{upper}}} \phi(E)\,dE} \equiv \sum_m N^m\,\sigma_{c_j}^m,$$

where

$$\sigma_{c_j}^m = \frac{\int_{E_{j_{lower}}}^{E_{j_{upper}}} \phi(E)\,\sigma_c(E)\,dE}{\int_{E_{j_{lower}}}^{E_{j_{upper}}} \phi(E)\,dE}.$$

Clearly the microscopic group cross sections have greater usefulness in that for reactor systems for which differences in corresponding intra-group spectral weightings are not important, they may be directly used by simple homogenization:

$$\Sigma_{c_j} = \sum_m N^m \sigma_{c_j}^m.$$

Analogous averaging formulas may be used for the quantities

$$(\nu\sigma_f)_j,\ \sigma_{f_j},\ \sigma_{el_j},\ \sigma_{in_j},\ \sigma_{el_{j\to k}},\ \sigma_{in_{j\to k}},\ \sigma_{total_j},$$

and others.

The detailed formula for $\sigma_{j\to k}$ or $\Sigma_{j\to k}$ for either elastic or inelastic cross sections is of the form

$$\sigma_{j\to k} = \frac{\displaystyle\int_{E_{k_{lower}}}^{E_{k_{upper}}} \left[\int_{E_{j_{lower}}}^{E_{j_{upper}}} \sigma_{el\ or\ inel}(E\to E')\phi(E)\,dE \right] dE'}{\displaystyle\int_{E_{j_{lower}}}^{E_{j_{upper}}} \phi(E)\,dE}.$$

The group diffusion constant

$$D_j = \frac{\displaystyle\int_{E_{j_{lower}}}^{E_{j_{upper}}} \phi(E)\,D(E)\,dE}{\displaystyle\int_{E_{j_{lower}}}^{E_{j_{upper}}} \phi(E)\,dE}$$

rigorously cannot be analogously obtained by averaging before homogenization because

$$D(E) = 1/3\Sigma_{transport}(E),$$

where

$$\Sigma_{transport}(E) = \sum_m N^m \sigma_{tr}(E).$$

In practice, however, the reciprocals of the individual elements are nevertheless often flux weighted with some assumed suitable intragroup spectrum:

$$\left(\frac{1}{\sigma^m_{tr}}\right)_j = \frac{\int_{E_{j_{lower}}}^{E_{j_{upper}}} \frac{\phi(E)\,dE}{\sigma^m_{tr}(E)}}{\int_{E_{j_{lower}}}^{E_{j_{upper}}} \phi(E)\,dE}.$$

Other microscopic group transport cross sections of the elements obtained by formulas such as

$$\sigma^m_{tr_j} \quad \frac{1}{\left(\frac{1}{\sigma^m_{tr}}\right)_j}$$

are subsequently homogenized:

$$\Sigma_{tr_j} = \sum_m N^m \sigma^m_{tr_j},$$

to obtain the macroscopic group transport cross section. The group diffusion parameter of the mixture is then taken to be $D_j = 1/3\Sigma_{tr_j}$ for diffusion-theory calculations. Estimates of errors and discussion of the difficulties encountered in evaluation of averaged diffusion constants for groups are given by Zweifel and Ball.[22] Further discussion of fast multigroup definitions may be found in Reactor Physics Constants.[8] Details of preparation of a multigroup set of cross sections are given by Yiftah, Okrent, and Moldauer.[23]

As will be later discussed, the reciprocal averaging of microscopic transport cross sections with subsequent homogenization can be especially in error for cases of mixtures of resonance structure materials.

The flux averaging of cross sections (or reciprocal cross sections for transport processes) is usually the averaging procedure employed to obtain the group constants for multiregion multigroup analyses. It is, however, neither the only weighting procedure suggested nor employed, and indeed in some cases, depending upon the reactor quantity calculated, it may not be the correct weighting procedure. In some cases weightings which consider also the adjoint may be preferable (see, for example, Refs. 24 and 25).

Another source of error in the flux averaging of the reciprocal transport cross section may arise if flux, ϕ, and current, $\vec{J}$, are not space

and energy separable (see, for example, Ref. 22). In this case, even though $\Sigma_{tr}(E)$ is independent of position in some region, Σ_{tr_j} in the region may be dependent upon position. This follows from

$$\Sigma_{tr_j}(\vec{r}) = \frac{\int_{\text{group } j} \vec{J}(\vec{r},E)\,\Sigma_{tr}(\vec{r},E)\,dE}{\int_{\text{group } j} \vec{J}(\vec{r},E)\,dE}.$$

Σ_{tr_j} is independent of $\vec{r}$ only if $\Sigma_{tr} = \Sigma_{tr}(E)$ and if $\vec{J}(\vec{r},E) = \vec{J}_r(\vec{r})\,J_E(E)$, i.e.,

$$\Sigma_{tr_j} = \frac{\int_{\text{group } j} J_E(E)\,\Sigma_{tr}(E)\,dE}{\int_{\text{group } j} J_E(E)\,dE}.$$

From $\phi(E,\vec{r}) = \phi_r(\vec{r})\,\phi_E(E)$ and Fick's law it follows that

$$\Sigma_{tr_j} = \frac{\int_{\text{group } j} \phi_E(E)\,dE}{\int_{\text{group } j} \frac{\phi_E(E)}{\Sigma_{tr}(E)}\,dE}.$$

A problem which frequently arises in multigroup calculations is that of the reduction of a many-group set to an equivalent fewer-group set. This may be necessitated in order to reduce computational time or to allow use of machine code programs which can employ at most a few groups. The latter frequently arises in multidimensional analyses. This reduction of groups is clearly related to the problems, just discussed, of the evaluation of group parameters.

For the analytically simple case of the calculation of the multigroup fluxes and the material buckling of a bare homogeneous system by diffusion theory, the requirements on the reduction procedures are that the material bucklings be unchanged (or k_{eff} if a geometrical buckling is assumed), that the individual group fluxes of the reduced case equal the sum of the equivalent group fluxes of the unreduced case, and that the reaction rates be unchanged. It may be shown that flux weighting satisfies these requirements. The reduction formulae are analogous to the flux-weighted group

evaluations previously discussed. Let J be the group designation of the reduced set. Then, for example, the homogenized capture cross section is given by

$$\Sigma_{c_J} = \frac{\sum_{j \text{ in } J} \phi_j \Sigma_{c_J}}{\sum_{j \text{ in } J} \phi_j},$$

where ϕ_j are the calculated fine group fluxes and "j in J" means fine groups comprising a coarse group J. The group transfer cross sections from coarse group J to coarse group K are obtained from the formula

$$\Sigma_{J \to K} = \frac{\sum_{j \text{ in } J} \sum_{k \text{ in } K} \phi_j \Sigma_{j \to k}}{\sum_{j \text{ in } J} \phi_j}.$$

The coarse-group diffusion constant is obtained from the equation

$$D_J = \frac{\sum_{j \text{ in } J} D_j \phi_j}{\sum_{j \text{ in } J} \phi_j}.$$

If the transport cross section rather than diffusion constant is required as a machine program input, then

$$\Sigma_{tr_J} = 1/3D_J.$$

In the event that it is desired to carry out an analysis in few-group systems other than that used in the specific reduction weighting, the reduction of the microscopic fine-group cross sections to coarse groups has practical advantages, although if the intracoarse-group spectra is too different then errors in coarse-group fluxes and material bucklings (or k_{eff} values) will not be negligible. Clearly, in addition, reduction of the reciprocals of the group microscopic transport cross sections of the fine groups before homogenization can lead to errors in D_J in analogy to the previous discussion.

An example of a flux spectral averaging and group-reduction code is GAM-I.[26]

VI. TRANSPORT CROSS SECTION

Previously we have considered the question of the homogenization of a mixture of materials. In particular we discussed the difficulties of the homogenization of group microscopic transport cross sections of elements to obtain the group macroscopic transport of mixtures.

The definition of transport cross section is closely related both to the degree of accuracy desired in the flux solutions and to the mode of solution employed. These considerations are especially important in fast systems because anisotropy of elastic scattering occurs also in the center of mass system. Furthermore, because the dimensions of the systems are often such that a mean free path represents a significant distance relative to the dimensions, transport methods of solution are frequently necessary. In addition, because of the necessity for considering many neutron energy groups, the question of the effect of reduction of group widths upon the definition of the transport cross section becomes a consideration.

The one-dimensional, monoenergetic, steady-state Boltzmann equation with the scattering cross section and flux expanded in Legendre polynomial series is

$$\mu \frac{\partial \phi(x,\mu)}{\partial x} + \Sigma_{\text{total}} \phi(x,\mu) = \sum_{\ell=0}^{\infty} \frac{2\ell+1}{2} \Sigma_{s\ell} P(\mu) \phi_\ell(x) + S(x),$$

where μ is the cosine of the angle between the x-direction and the neutron flux direction, and S(x) represents an isotropic source distribution. Recall that

$$\Sigma_{s\ell} = \int_{-1}^{+1} \Sigma_s(\mu_0) P_\ell(\mu_0) d\mu_0,$$

where $\Sigma_s(\mu_0)$ is the scattering cross section in the laboratory system for an incident and scattered neutron having direction cosine μ_0, and that the $\phi_\ell(x)$ are related to the $\phi(x,\mu)$ by the relation

$$\phi(x,\mu) = \sum_{\ell=0}^{\infty} \frac{2\ell+1}{2} \phi_\ell(x) P_\ell(\mu).$$

Information on angular distributions has in most cases confirmed the compound-nucleus nature of inelastic scattering, i.e., in the center-of-mass system the neutrons are isotropically scattered. The effect of angular distribution in the laboratory system of inelastically scattered neutrons can be

neglected, except for very light nuclei. For the energy range of fast neutrons it is important to consider both the elastic-scattering anisotropy in the center-of-mass and the anisotropy due to transformation from the center-of-mass to the laboratory system. Thus, although Σ_s can be considered replaceable by $(\nu\Sigma_f + \Sigma_{in} + \Sigma_s)$ in practice Σ_s and Σ_{in} are generally taken as isotropic, and only the anisotropic-containing elastic scattering, Σ_s, need be considered in the argument to follow.

By consideration of terms $\ell \leq 1$ in the flux and flux gradient,

$$\phi(x,\mu) = \frac{\phi_0(x)}{2} + \frac{3}{2}\,\phi_1(x)P_1(\mu)$$

and

$$\frac{\partial\phi}{\partial x} = \frac{1}{2}\,\frac{d\phi_0(x)}{dx} + \frac{3}{2}\,\frac{d\phi_1(x)}{dx}\,P_1(\mu),$$

the transport equation becomes

$$\frac{\mu}{2}\frac{d\phi_0}{dx} + \frac{3}{2}\,\mu\,\frac{d\phi_1}{dx}\,P_1(\mu) + \frac{\Sigma_{tot}}{2}\,\phi_0 + \frac{3}{2}\,\Sigma_{tot}\,\phi_1 P_1(\mu)$$

$$= \frac{\Sigma_s}{2}\,\phi_0 + \frac{3}{2}\,\Sigma_{s_1}\,P_1(\mu)\,\phi_1,$$

where S (x) is assumed to be zero and where

$$\Sigma_{s_1} = \int_{-1}^{+1} \mu_0\,\Sigma_s(\mu_0)\,d\mu_0 = \overline{\mu}_0\;\Sigma_s.$$

Multiplication by P_0 and integration over μ, and subsequently by P_1 and integration over μ, give the two coupled differential equations of the P_1 approximation:[27]

$$\frac{d\phi_1}{dx} + \Sigma_{tot}\,\phi_0 = \Sigma_s\,\phi_0$$

and

$$\frac{1}{3}\frac{d\phi_0}{dx} + \Sigma_{tot}\,\phi_1 = \Sigma_{s_1}\,\phi_1.$$

The assumed linear flux dependence thus require linear scattering information. Furthermore, the coupled set reduces directly to the form of a coupled set for the case of only isotropic scattering if in the latter set:

$$\frac{d\phi_1}{dx} + \Sigma_{tot}\,\phi_0 = \Sigma_{s_0}\,\phi_0$$

and

$$\frac{1}{3}\,\frac{d\phi_0}{dx} + \Sigma_{tot}\,\phi_1 = 0,$$

there is substituted

$$\Sigma_{tot} \rightarrow \Sigma^*_{tot} = \Sigma_{tot} - \Sigma_{s_1} \equiv \Sigma_{tot} - \bar{\mu}_0\,\Sigma_s$$

and

$$\Sigma_{s_0} \rightarrow \Sigma^*_{s_0} = \Sigma_{s_0} - \Sigma_{s_1} \equiv \Sigma_s - \bar{\mu}_0\,\Sigma_s.$$

Usually Σ^*_{tot} is the definition of transport cross section used in construction of multigroup parameters. The latter substitutions are referred to as the "transport approximation." Clearly it contains sufficient anisotropic cross-section information if flux solutions up to an accuracy of two terms in the flux and current Legendre expansions are desired. In addition, as is well-known, for the case of monoenergetic neutrons (one-group set) the isotropic scattering P_1 equations reduce to the one-group diffusion equations:

$$-\frac{1}{3\Sigma^*_{tot}}\,\frac{d^2\phi_0}{dx^2} + \Sigma^*_{tot}\,\phi_0 - \Sigma^*_s\,\phi_0 = 0.$$

More explicitly,

$$-\frac{1}{3[\Sigma_{tot} - \bar{\mu}_0\Sigma_s]}\,\frac{d^2\phi_0}{dx^2} + [\Sigma_{tot} - \Sigma_s]\,\phi_0 = 0.$$

As fast reactor analyses often require flux solutions of higher order than the P_1 component, the question arises as to whether the transport approximation (i.e., P_1 in scattering) is or is not in practice sufficiently accurate also if solutions having higher moments of flux and current are desired.[28]

Furthermore, the general need for multigroups introduces the question of the validity of the previous one-group definition of transport cross section.

The corresponding multigroup P_1 flux and current equations obtainable from a multigroup form of the transport equation are

$$\frac{d\phi_j^1(x)}{dx} + \Sigma_{tot_j}\,\phi_j^0(x) = \sum_{\text{all } j'} \Sigma^0_{s_{j'\to j}}\,\phi_{j'}^0(x)$$

and

$$\frac{1}{3}\,\frac{d\phi_j^0(x)}{dx} + \Sigma_{tot_j}\,\phi_j^1(x) = \sum_{\text{all } j'} \Sigma^1_{s_{j'\to j}}\,\phi_{j'}^1(x).$$

The summation in the second equation is seen to include the anisotropic scattering components transferred from other groups. Use of these multigroup equations for this reason is referred to as the consistent P_1 approximation.[27,30]

The corresponding multigroup equations for the case of isotropic scattering are

$$\frac{d\phi_j^1(x)}{dx} + \Sigma_{tot_j}\,\phi_j^0(x) = \sum_{\text{all } j'} \Sigma_{s_{j'\to j}}\,\phi_{j'}^0(x)$$

and

$$\frac{1}{3}\,\frac{d\phi_j^0(x)}{dx} + \Sigma_{tot_j}\,\phi_j^1(x) = 0.$$

The previous consistent P_1 multigroup equations can thus be brought into the form of the above P_0 equations only if in the summation on the right side of the second P_1 equation the anisotropic scattering transfer of other groups is considered negligible, i.e., $\Sigma^1_{s_{j'\to j}} = 0$ except for $\Sigma^1_{s_{j\to j}}$. Then the form of the isotropic equations are obtained by the transport approximation redefinitions:

$$\Sigma^*_{tot_j} = \Sigma_{tot_j} - \bar{\mu}_{0_j}\Sigma_{s_j}$$

and

$$\Sigma^{*}_{s_{j\to j'}} = \Sigma_{s_{j'\to j}} - \bar{\mu}_{0_j}\Sigma_{s_j}\,\delta_{j',j}.$$

In addition, there is then directly obtainable the multigroup diffusion equations of the form

$$-\frac{1}{3(\Sigma_{tot_j} - \bar{\mu}_{0_j}\Sigma_{s_j})}\frac{d^2\phi^0}{dx^2} + (\Sigma_{tot_j} - \Sigma_{s_j})\,\phi^0_j = \sum_{j'\neq j}\Sigma_{s_{j'\to j}}\phi^0_{j'}.$$

The corresponding spherical geometry form of the multigroup consistent P_1 equations are given in Ref. 28.

Thus, transport-theory codes which assume only isotropic scattering can be directly used, by use of the transport approximation, to solve the one-group P_1 equations which give scalar fluxes identical to diffusion theory if the transport approximation is also used in the diffusion theory solution. If only up to linear scattering is important, then one-group transport-theory codes which assume isotropic scattering can also be used to obtain higher-order flux and current components than P_1.

If multigroup transport-theory codes are used and isotropic scattering is assumed, the corresponding comments apply only if in addition the P_1 scattering anisotropy into other groups is neglected.

If in an energy-dependent (multigroup) case the energy loss per collision is large and/or if the group intervals are small, then the anisotropic scattering into other groups cannot necessarily be a priori neglected. It may be noted that in some recent multigroup reactor codes (Elmoe[30] and Gam[26]) containing a very large number of very small energy intervals that the anisotropic scattering into other groups is considered. These codes at the present are, however, used primarily to obtain fine, detailed flux spectra for cases of spatially independent spectra cases for subsequent use in calculation of fewer-group cross section sets for spatially dependent cases.

Pendlebury and Underhill[28] have empirically looked into the question of the adequacy of using either lower-order scattering-anisotropy information or the transport approximation in transport calculations for higher-order flux solutions. For a series of fast reactor calculations with scattering anisotropy to lower groups neglected, they find that it is not necessary to use $\ell > 5$ in scattering information, and that either $\ell = 1$ or the transport approximation often give results of acceptable accuracy. For example, in calculation of Godiva (the Los Alamos bare U^{235} spherical critical) the percent difference in use of the transport approximation relative to $\ell = 5$ scattering information is of the order of $\frac{1}{4}\%$ in radius with either an S_4 or S_8 flux solution by the SNG method. (S_4 and S_8 are different orders of flux approximations as obtained by the SNG transport method of solution; this will be discussed in a subsequent section.)

On the other hand, Joanou and Kazi,[29] have reported that, although errors in use of transport approximations are small for the bare sphere, such errors are more appreciable for the reflected systems reported. In some cases the differences between transport approximations and more exact methods were quite significant.

A definition of the group transport cross section often used in transport approximation with diffusion theory and with higher flux component calculations by transport codes is

$$\sigma_{tr_j} = \sigma_{c_j} + \sigma_{F_j} + \sigma_{el_{j\to k}} + \sigma_{in_{j\to k}} + \sigma_{el_{j\to j}} (1 - \bar{\mu}_{el_j}) + \sigma_{in_{j\to j}} (1 - \bar{\mu}_{in_j}),$$
$$j\neq k \qquad j\neq k$$

where the $\bar{\mu}$ are the average cosine of the scattering distribution in the laboratory system. As the fast reactor materials are generally not very light elements, the inelastic scattering is generally taken to be isotropic in the laboratory system. Because the elastic scattering can be anisotropic in the center-of-mass system at fast reactor energies, the scattering-anisotropy constant $\bar{\mu}_{el}$ is retained. Then,

$$\sigma_{tr_j} = \sigma_{c_j} + \sigma_{F_j} + \sigma_{in_j} + \sigma_{el_j} - \bar{\mu}_{el_j}\ \sigma_{el_j},$$

which is equivalent to the definition used by Yiftah et al.,[23] in their analysis of a fast reactor cross-section set. The importance of elastic-scattering anisotropy in other than very light elements can be seen in Table VI by comparisons of the values of 2/3A, for the case of isotropic center of mass scattering, with evaluated $\bar{\mu}$ values at 0.5 MeV in the laboratory system.

Table VI

ELASTIC-SCATTERING ANISOTROPIES IN THE LABORATORY SYSTEM COMPARED WITH VALUES OF 2/3A

($\bar{\mu}$ at 0.5 MeV from Ref. 28)

Material	U	Fe	C
2/3A	0.0028	0.012	0.056
$\bar{\mu}$	0.315	0 201	0.056

The large dependence of $\bar{\mu}$ upon neutron energy is evident when one considers that in going from E = 0.5 MeV to 2.0 MeV to 4.0 MeV in the case of carbon that $\bar{\mu}$ goes from 0.056 to 0.200 to 0.032 ($\bar{\mu}$ values from Ref. 28).

VII. TRANSPORT SOLUTIONS BY DISCRETE ORDINATE METHODS

Large digital computers have increased the application of discrete ordinate methods of solution of the transport equation. Familiarity with the method of spherical harmonics[27] is assumed so that correspondence of the two types of solutions can be made.

The two aspects of particular interest and both basic in solution by discrete ordinate methods are:

(1) determination of the angular distribution of the flux by solution of the transport equation for various particular directions;

(2) integration of the angular flux, to obtain the scalar flux, by a method of numerical quadrature wherein a weighted summation replaces the integration.

The slab-geometry, one-dimensional, monoenergetic, transport equation with isotropic scattering and isotropic sources is

$$\mu \frac{\partial \phi}{\partial x}(x,\mu) + \Sigma \phi(x,\mu) = \Sigma_s \frac{1}{2} \int_{-1}^{+1} \phi(x,\mu) d\mu + S(x).$$

The "discrete direction" methods stem from the Wick-Chandrasekhar method[27] in which the set of k equations for discrete directions, μ_k, of the form

$$\mu_k \frac{\partial \phi}{\partial x}(x,\mu_k) + \Sigma \phi(x,\mu_k) = \Sigma_s \sum_{\text{all } k} R_k \phi(x,\mu_k)$$

replaces the previous equation and where the original angular integral of the transport equation

$$\int_{-1}^{+1} \phi(x,\mu) d\mu \cong \sum_k R_k \phi(x,\mu_k),$$

wherein the quadrature parameters R_k and μ_k are those of the Gaussian quadrature formula. Recall that the latter means that the μ_k are $(L+1)$ in number and are the roots of the $P_{L+1}(\mu) = 0$ in the L'th approximation. The weights R_k are also $(L+1)$ in number and may be obtained from solution of the $(L+1)$ linear equations[31]

$$n = 0: \quad 2 = R_1 + R_2 + \ldots + R_{L+1};$$

$$n = 1: \quad 0 = R_1\mu_1 + R_2\mu_2 + \ldots;$$

$$\vdots$$

$$n: \quad \left[\frac{1}{n+1} - \frac{(-1)^{n+1}}{n+1}\right] = R_1\mu_1^n + R_2\mu_2^n + \ldots$$

For example, if the L = 1 parameters are desired, then $P_2(\mu) = 0$ for $\mu_1 = +0.577$ and $\mu_2 = -0.577$, and the weights follow from simultaneous solution of the pair

$$2 = R_1 + R_2;$$

$$0 = 0.577\ R_1 - 0.577\ R_2,$$

from which $R_1 = R_2 = 1$.

For the case L = 7, there are four positive and four negative directions, and eight weights. The parameters are approximately[31]

$$|\mu_k| = 0.960,\ 0.797,\ 0.526, \text{ and } 0.183,$$

with

$$R_k = 0.101,\ 0.222,\ 0.314 \text{ and } 0.363,$$

respectively.

The scalar flux in the slab obtainable by the Wick-Chandrasekhar method with Gaussian quadrature weights and directions can be shown to be identical with that obtainable by use of the spherical harmonics solution of order P_L.[32] In a similar manner, the use of double Gaussian quadrature in the intervals $\mu = 0$ to 1 and $\mu = -1$ to 0 is the analog of the double spherical harmonics method of Yvon.[27] It is especially useful in cases of angular flux discontinuity at $\mu = 0$, as is frequently encountered in slab-geometry cells. For comparison the 8-angle double Gaussian quadratue parameters are approximately[33]

$$|\mu_k| = 0.931,\ 0.670,\ 0.330, \text{ and } 0.0694$$

with

$$R_k = 0.174,\ 0.326,\ 0.326 \text{ and } 0.174,$$

respectively. This corresponds to a Yvon double P_3.

Many quadrature formulas exist. In the Westinghouse "RANCH" code,[34] for example, one may either use the internally available double Gauss parameters up to 12 angles or supply any other quadrature parameters as input. RANCH is a one-energy group IBM-704 transport code in slab geometry using a discrete method.

The one-dimensional multigroup transport codes which have been much used are the Los Alamos SNG[35] and DSN[36] codes. They enable transport solutions of various approximations for sphere, slab, and infinite-cylinder geometries. The SNG code preceded the DSN (Discrete SN) code. Neither code is, however, strictly a discrete ordinate solution in the sense of the Wick equation. Both utilize the technique of dividing the μ space into finite directions having definite weights. The manner of arriving at the quadrature formulae differ, and the handling of the directions in the transport equation differ. In this regard the DSN code is closer to the discrete ordinate method.

The SNG method divides $\mu = -1$ to $+1$ into equal $\Delta\mu$ intervals. The approximation S_6 has 6 divisions and 7 directions. The angular flux distribution between these directions is generally assumed linear in μ. Two of the directions are always $\mu = +1$ and -1 and, generally, $\mu = 0$ is also a direction.

Consider the one-dimensional spherical case. The angular flux $\phi(r,\mu)$ between μ_{j-1} and μ_j is then

$$\phi(r,\mu) = \left[\frac{\mu-\mu_{j-1}}{\mu_j-\mu_{j-1}}\right]\phi(r,\mu_j) + \left[\frac{\mu_j-\mu}{\mu_j-\mu_{j-1}}\right]\phi(r,\mu_{j-1})$$

$$= \frac{n}{2}\left[(\mu-\mu_{j-1})\,\phi(r,\mu_j) + (\mu_j-\mu)\phi(r,\mu_{j-1})\right],$$

where n is the number of equal $\Delta\mu$ intervals in region $-1 \le \mu \le +1$. The integral for the total flux is then

$$\Phi(r) = \frac{1}{2}\int_{-1}^{+1}\phi(r,\mu)\,d\mu = \frac{1}{2}\sum_{j=1}^{n}\int_{\mu_{j-1}}^{\mu_j}\left(\frac{n}{2}\right)\left[(\mu-\mu_{j-1})\phi(r,\mu_j) + (\mu_j-\mu)\phi(r,\mu_{j-1})\right]d\mu$$

$$= \frac{1}{2n}\,\phi(r,\mu_0) + \sum_{j=1}^{n-1}\frac{1}{n}\,\phi(r,\mu_j) + \frac{1}{2n}\,\phi(r,\mu_n).$$

Thus the assumption of equal intervals and linearity within intervals lead to a quadrature formula having equal weighted interval directions and half-weighted end points.

The group spatial differential equation is written as

$$\left(\mu \frac{\partial}{\partial r} + \frac{1 - \mu^2}{r} \frac{\partial}{\partial \mu} + \Sigma_j \right) \phi_j(r,\mu) = S_j(r),$$

where it is understood that $S_j(r)$ includes also the scattering sources within group j and transferred into group j. Insertion of the linearity flux function between μ_{j-1} and μ_j and integration out of the μ dependence by integration from μ_{j-1} to μ_j give a set of n nonpartial differential equations for each group. The latter equations are coupled by the directions μ_{j-1} and μ_j. Thus, for one of the groups,

$$\left(a_j \frac{d}{dr} + \frac{b_j}{r} + \Sigma \right) \phi(r,\mu_j) + \left(\bar{a}_j \frac{d}{dr} - \frac{b_j}{r} + \Sigma \right) \phi(r,\mu_{j-1}) = 2S(r),$$

where the constants are functions only of the $\Delta\mu$ interval endpoints. (The factor 2 results from $\int_{-1}^{+1} d\mu = 2$).

The n + 1 direction is that corresponding to $\mu = -1$, and the solution is obtained directly from the transport equation

$$\left(-\frac{d}{dr} + \Sigma \right) \phi(r,-1) = S(r)$$

for each group. Thus, in the n-approximation there are n + 1 angular flux directions obtained.

It is evident that because of the assumption of linearity between these directions, in the case of problems having solutions with complete linearity in the interval -1 to +1 then the same scalar flux as given by diffusion theory is obtained. Thus, for problems in which diffusion theory gives accurate scalar flux solutions, the SNG method gives identical results in S_2 and all higher approximations.

Though not shown here, in the SNG method the equations of neutron balance are conserved.[37]

Comparisons of critical core radius calculations by the transport approximation with S_4 and diffusion theory have been reported[5] for a series of fast systems. The multigroup analyses are reproduced in Fig. 9. It is noted that diffusion theory, because of greater calculated leakage, lead

to larger radii for criticality relative to S_4. It should be remembered that errors in radii must be multiplied by factor three to estimate critical mass errors and that variations from the curve can occur depending upon the composition and configuration of a critical system. It may be possible in some instances that diffusion theory may lead to smaller core sizes if, for example, a reflector significantly modifies the spectrum toward larger reactivities.

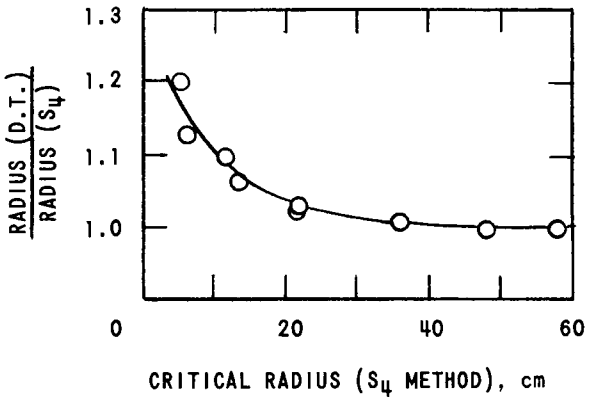

Fig. 9

Ratio of Critical Radii (Diffusion Theory to S_4 Method) as a Function of Critical Radius by S_4 Method (from Ref. 5)

A comparison of various orders of SNG approximations have been reported[38] for a solid plutonium sphere assembly. The percent error in critical radius is shown in Fig. 10. It is noted that with higher SNG approximations the calculated critical masses increase. Yiftah et al., have calculated the Los Alamos Popsy assembly with both S_4 and S_8. Popsy is essentially a 4.5-cm-radius plutonium core with 9.5-in. natural uranium reflector. The approximation S_4 gave 5.03 kg for the critical mass whereas S_8 gave 5.18 kg. In other words S_4 gave a mass smaller by about 3%, which indicates a radius smaller by about 1%. For comparison, however, the experimental mass is about 5.78 kg.

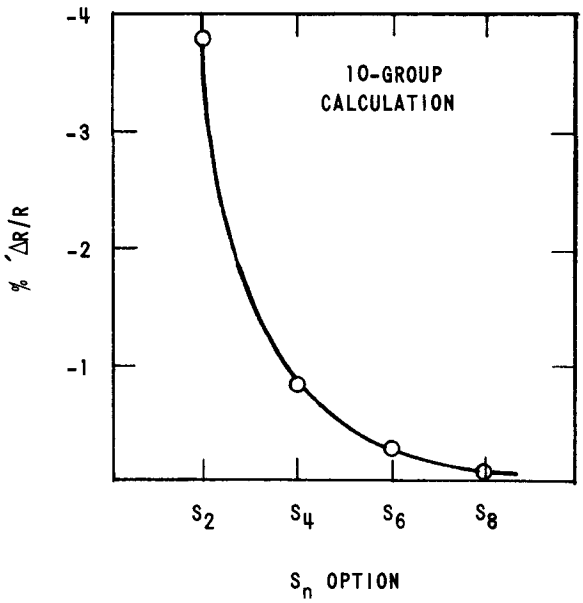

Fig. 10

Relative Percent Error in Critical Radius as a Function of SNG Option (from Ref. 38)

VIII. DISCRETE S_N (DSN) METHOD

The question might be raised as to why have the DSN method when so much of what is desired is apparently fulfilled by the SNG method.

The SNG method was believed to be somewhat strict in its initial assumption of linearity. A reason then was to see if a method based on more general and less stringent initial assumptions would lead to a simple and more flexible method of solution. Furthermore, some practical difficulties have also been observed with the SNG; for example, the flux solutions for thin-slab cells have in some instances been unsymmetrical. In addition, the presence of the direction $\mu = 0$ may give rise to convergence difficulties in cases of important tangential flux-discontinuity effects.

It might also be asked: why not just use the Wick method previously referred to? It was quite general and need not necessarily be restricted to Gaussian quadrature. The reason is largely the difficulty in practice for the cases of non-slab geometries as, for example, spherical, to handle accurately by difference methods the term

$$\frac{1 - \mu^2}{r} \frac{\partial \phi}{\partial \mu} (r, \mu)$$

by means of the $\phi_k(r, \mu_k)$ of the Wick method. The SNG method circumvents this difficulty by the integration over the $\Delta\mu_j$ intervals assuming linearity in μ and subsequently operating with the angular fluxes at the end points of the $\Delta\mu_k$.

The following development argument of the DSN method follows essentially that given by Carlson and Bell.[37]

In the DSN method an assumed form,

$$\left(a_k \frac{d}{dr} + \frac{b_k}{r} + \Sigma\right) \phi(r, \mu_k) + \left(\bar{a}_k \frac{d}{dr} - \frac{b_k}{r} + \Sigma\right) \phi(r, \mu_{k-1}) = 2S(r),$$

similar to that obtained in the SNG method, is taken. The parameters a_k, b_k, and $\bar{a}_k$ are not defined. The equation is transformed into a form having a smaller number of parameters. The μ_k and μ_{k-1} again signify a priori chosen end points of chosen $\Delta\mu_k$ intervals. In addition, values of $\bar{\mu}_k$ are also a priori chosen, such that

$$\mu_{k-1} \leq \bar{\mu}_k \leq \mu_k.$$

The previous equation may be re-written as

$$\left[a_k \frac{d\phi}{dr}(r,\mu_k) + \bar{a}_k \frac{d\phi}{dr}(r,\mu_{k-1})\right] + \frac{b_k}{r}\left[\phi(r,\mu_k) + \phi(r,\mu_{k-1})\right]$$

$$+ \Sigma\left[\phi(r,\mu_k) + \phi(r,\mu_{k-1})\right] - 2\frac{b_k}{r}\phi(r,\mu_{k-1}) = 2S(r)$$

by addition and subtraction of b_k/r on the left side. The argument is that more generally the equation may take the form

$$A_k \frac{d\phi}{dr}(r,\bar{\mu}_k) + \frac{B_k}{r}\phi(r,\bar{\mu}_k) + \Sigma\phi(r,\bar{\mu}_k) - \frac{B_k}{r}\phi(r,\mu_{k-1}) = S(r),$$

where $A_k \equiv \bar{\mu}_k$. $\bar{\mu}_k$ is the chosen discrete direction between μ_{k-1} and μ_k, and B_k is obtained by imposing the property of neutron conservation. Neutron conservation requires that for each energy group the equation

$$\left(\frac{d}{dr} + \frac{2}{r}\right)J(r) + \Sigma\phi(r) = S(r)$$

holds, where the group current is given by

$$J(r) = \frac{1}{2}\sum_{k=1}^{n} (\Delta\mu)_k \bar{\mu}_k \phi(r,\bar{\mu}_k)$$

and the scaler flux is given by

$$\phi(r) = \frac{1}{2}\sum_{k=1}^{n} (\Delta\mu)_k \phi(r,\bar{\mu}_k).$$

In this manner it was determined that

$$B_k = 2\left[\bar{\mu}_k - \frac{2}{(\bar{\mu}_k - \mu_{k-1})}\sum_{k=1}^{n} \frac{1}{2}(\Delta\mu)_k \bar{\mu}_k\right].$$

The $\bar{\mu}_k$ are the chosen k'th discrete directions, and the $(\Delta\mu)_k$ is the quadrature weight chosen for the k'th ordinate.

To start the angular iterative process for a group $\phi(r,\mu_{k-1})$ for k = 1, i.e., $\phi(r,\mu_0) \equiv \phi(r, -1)$, is obtained from the original group transport equation with $\mu = -1$:

$$-\frac{\partial\phi}{\partial r}(r, -1) + \Sigma\phi(r, -1) = S(r).$$

From $\phi(r, -1)$ is then obtained $\phi(r, \bar{\mu}_1)$ by means of the DSN equation. A linear extrapolation,

$$\phi(r, \mu_k) = \left[\frac{\phi(r, \bar{\mu}_k) - \phi(r, \mu_{k-1})}{\bar{\mu}_k - \mu_{k-1}} \right] (\mu_k - \mu_{k-1}) + \phi(r, \bar{\mu}_{k-1}),$$

is then used to obtain the spatial distribution of the angular flux at the right end point of the $(\Delta \mu)_1$ angular interval for subsequent use in the DSN formula, etc.

Although the method may use any quadrature formula, from the point of view of neutron migration it is satisfying if the group scalar fluxes obtained by all orders of approximation of the DSN method result in the same fluxes as given by diffusion theory for problems in which diffusion theory is adequate. Recall that SNG satisfied this requirement automatically through choice of linearity of angular flux between interval endpoints. Considering that with linearity of angular flux, as required by diffusion theory, $\phi(\mu) \sim \mu$, then the current is

$$J = \frac{1}{2} \int_{-1}^{+1} \mu^2 \, d\mu = \frac{1}{3},$$

which places a requirement on initial choice of quadratures or an adjustment of quadrature parameters in DSN so that analogously

$$\frac{1}{2} \sum_{k=1}^{n} (\Delta \mu)_k (\bar{\mu}_k)^2 = \frac{1}{3}.$$

In the DSN codes as often used the $(\Delta \mu)_k$ intervals (weights) are chosen equal and even in number. The μ_k (discrete directions) are chosen approximately to be at the midpoints of the $(\Delta \mu)_k$. They deviate from the exact midpoints by some small common factor which is analytically determined so as to insure the previous desirable correspondence with diffusion theory. For example, for the S_4 sphere case, the $\bar{\mu}_k$ values[39] are -0.7745966, -0.2581989, +0.2581989, and +0.7745966, which are seen to differ from the exact midpoint values -0.75, -0.25, +0.25, and +0.75 by a factor ~1.0328.

Another modification to insure the 1/3 current factor has been the use of a constant small incremental shift in the midpoint positions.[37]

It is informative to briefly list here some of the usual problem types solved by the DSN method. As normally coded, it is applicable to

n = 2, 4, 6, 8, or 16-order approximations in plane, infinite cylinder, and spherical geometries. Adjoint solutions are also obtainable.

1. Obtain k_{eff}, given dimensions and compositions.
2. Obtain concentrations of specified materials for criticality, given dimensions and compositions.
3. Obtain dimensions of particular regions for criticality, given dimensions and compositions.
4. Obtain the exponential rate (α) on the assumption that the flux is separable with respect to time, with time variation exp (α t).

Among options, various boundary conditions may be imposed at the central and outer boundaries. Outer boundary condition options are zero inward flow, perfect reflection, and slab periodicity. For slabs there are on the inner (left) boundary in addition to perfect reflection also the free-boundary and periodic-boundary conditions. "Periodic boundary" denotes the condition where the angular distribution at one slab boundary equals the angular distribution at the other slab boundary as required in some slab-cell calculations.

A 2-dimensional DSN program is TDC for R-Z geometry calculations.[36,37]

IX. B_N METHOD AND ASYMPTOTIC DIFFUSION THEORY

During discussion of multigroup diffusion theory it was noted that in the event that the system is bare and homogeneous, analysis of material buckling and flux could be rather simply carried out even by hand. Furthermore, as discussed, the transport approximation can be used in case of linear scattering, subject, of course, to the assumption that anisotropic scattering into other groups can be neglected. In both the P_1 approximation and in the corresponding diffusion-theory solutions, only angular flux distributions up to linear anisotropy are accounted for. Situations arise, however, in which flux anisotropy higher than linear must be considered even though the assumption of linear scattering may be sufficient. These considerations lead to the so-called consistent B_1 and B_1 approximations[40] in analogy with the consistent P_1 and P_1 approximations. Corresponding to the analysis of fundamental (normal) mode diffusion theory there is obtained an analysis by fundamental mode asymptotic diffusion theory.[5,30] The latter is a solution which contains all orders of flux anisotropy in the solution of the scalar flux. Important for fast reactor multigroup analyses is that the group scalar fluxes and material bucklings may be more accurately obtained for the central regions, assuming of course that the cross-section parameters are sufficiently well-known.

The one-dimensional, monoenergetic, slab-geometry, transport equation is

$$\mu \frac{\partial \phi}{\partial x}(x,\mu) + \Sigma \phi(x,\mu) = \int \Sigma_s(\mu' \to \mu)\, \phi(x,\mu')\, d\mu' + \frac{S(x)}{2},$$

where $\phi(x,\mu)d\mu$ is the flux between μ and $d\mu$, and $S(x)$ is assumed to be isotropic in the laboratory system.

Rather than expanding ϕ and Σ_s in Legendre series, the Fourier transforms

$$\overline{\phi}(B,\mu) = \frac{1}{\sqrt{2\pi}} \int_{-\infty}^{+\infty} \phi(x,\mu)\, e^{iBx}\, dx,$$

$$\overline{S}(B) = \frac{1}{\sqrt{2\pi}} \int_{-\infty}^{+\infty} S(x)\, e^{iBx}\, dx,$$

$$\phi(x,\mu) = \frac{1}{\sqrt{2\pi}} \int_{-\infty}^{+\infty} \overline{\phi}(B,\mu)\, e^{-iBx}\, dB,$$

and

$$S(x) = \frac{1}{\sqrt{2\pi}} \int_{-\infty}^{+\infty} \overline{S}(B)\, e^{-iBx}\, dB$$

are employed.

Multiplication of the transport equation by e^{iBx} and integration of all terms between $-\infty$ and $+\infty$ with respect to x give

$$\mu \int_{-\infty}^{+\infty} e^{iBx} \frac{\partial \phi}{\partial x}(x,\mu)\, dx + \Sigma \int_{-\infty}^{+\infty} e^{iBx}\, \phi(x,\mu)\, dx =$$

$$\int_{\mu'} \Sigma_s(\mu' \rightarrow \mu) \int_{-\infty}^{+\infty} e^{iBx}\, \phi(x,\mu')\, dx\, d\mu' + \int_{-\infty}^{+\infty} \frac{S(x)}{2}\, e^{iBx}\, dx.$$

By integration by parts of the first integral and expressing in terms of transforms, the equation may be cast in the form

$$\Sigma \overline{\phi}(B,\mu)\left[1 - \frac{i\mu B}{\Sigma}\right] = \int_{\mu'} \Sigma_s(\mu' \rightarrow \mu)\, \overline{\phi}(B,\mu')\, d\mu' + \frac{\overline{S}(B)}{2}.$$

Assume isotropic scattering in the laboratory system, i.e., for B_0 approximation, which is the case presently of interest. Hence, substituting

$$\Sigma_S = \int_{-1}^{+1} \Sigma_s\, d\mu' = 2\Sigma_s$$

and

$$\overline{\phi}_0(B) = \int_{-1}^{+1} \overline{\phi}(B,\mu')\, d\mu'$$

into the previous equation and then dividing by the quantity in brackets gives

$$\Sigma\bar{\phi}(B,\mu) = \frac{\Sigma_S\,\bar{\phi}_0(B)}{2\left[1 - \frac{i\mu B}{\Sigma}\right]} + \frac{\bar{S}(B)}{2\left[1 - \frac{i\mu B}{\Sigma}\right]}.$$

Insertion of the Legendre expansion,

$$\bar{\phi}(B,\mu) = \sum_{\ell=0}^{\infty} \frac{2\ell+1}{2}\,\bar{\phi}_\ell(B)\,P_\ell(\mu),$$

into the left side of the equation, multiplication of both sides by $P_j(\mu)$, and integration with respect to μ give

$$\Sigma \int_{-1}^{+1} \left[P_j(\mu) \sum_{\ell=0}^{\infty} \frac{2\ell+1}{2}\,\bar{\phi}_\ell(B)\,P_\ell(\mu)\right] d\mu =$$

$$\Sigma_S\,\bar{\phi}_0\left[\frac{1}{2}\int_{-1}^{+1} \frac{P_j(\mu)}{\left(1 - \frac{i\mu B}{\Sigma}\right)}\,d\mu\right] + \bar{S}(B)\left[\frac{1}{2}\int_{-1}^{+1} \frac{P_j(\mu)}{\left(1 - \frac{i\mu B}{\Sigma}\right)}\,d\mu\right].$$

As only the j'th integrated term is non-zero, the $\bar{\phi}_j(B)$ of the B_0 approximation is

$$\Sigma\bar{\phi}_j(B) = \left[\Sigma_S\,\bar{\phi}_0(B) + \bar{S}(B)\right]A_{j,0},$$

where

$$A_{j,0} = \frac{1}{2}\int_{-1}^{+1} \frac{P_j(\mu)}{\left(1 - \frac{i\mu B}{\Sigma}\right)}\,d\mu.$$

(The corresponding coefficients for the B_n approximation are given by

$$A_{j,\ell} = \frac{1}{2}\int_{-1}^{+1} \frac{P_j(\mu)\,P_\ell(\mu)}{\left(1 - \frac{i\mu B}{\Sigma}\right)}\,d\mu,$$

where $\ell = n$.)

$\bar{\phi}_0(B)$, which is the transform of the scalar flux, is then obtained from

$$\Sigma\bar{\phi}_0(B) = \Sigma_S \bar{\phi}_0(B) A_{00} + \bar{S}(B) A_{00},$$

which may be written explicitly as

$$\bar{\phi}_0(B) = \frac{\bar{S}(B)}{\frac{B}{\tan^{-1}\left(\frac{B}{\Sigma}\right)} - \Sigma_S},$$

for

$$A_{00} = \frac{\Sigma}{B} \tan^{-1}\left(\frac{B}{\Sigma}\right).$$

In terms of absorption cross section $\Sigma_A = \Sigma - \Sigma_S$, the previous expression for $\bar{\phi}_0(B)$ takes the form

$$\bar{\phi}_0(B) = \frac{\bar{S}(B)}{\Sigma_A + \left[\frac{B}{\tan^{-1}\left(\frac{B}{\Sigma}\right)} - \Sigma\right]}.$$

The above is the asymptotic diffusion-theory equation, and the quantity in brackets is the asymptotic transport leakage term corresponding to $B^2/3\Sigma$ of diffusion theory, where B^2 is the buckling.[5,30] In cases where B^2 is negative (i.e., $k_\infty < 1$), then $\sqrt{-B^2} = iB$ and the bracketed expression contains $\tanh^{-1}$ rather than $\tan^{-1}$. Negative B^2 are encountered, for example, in the calculation of the equilibrium spectrum in natural uranium and in fast reactor blankets sufficiently distant from core neutron sources.

For small values of B/Σ,

$$\tan^{-1}\left(\frac{B}{\Sigma}\right) \simeq \frac{B}{\Sigma} - \frac{B^3}{3\Sigma^3} + \frac{B^5}{5\Sigma^5},$$

so that

$$\lim_{\frac{B}{\Sigma}\to 0} \left[\frac{B - \Sigma\tan^{-1}\left(\frac{B}{\Sigma}\right)}{\tan^{-1}\left(\frac{B}{\Sigma}\right)}\right] = \frac{B^2}{3\Sigma}.$$

Application of asymptotic diffusion theory to the case of linear scattering may be made by substitution of transport cross section for the total cross section.

Extension of asymptotic theory to multigroup fundamental mode analyses for spectral and buckling analyses is evident by analogy with the previously described diffusion-theory normal-mode calculations.

As an example of the method and to indicate the order of magnitude of the deviations between diffusion theory and asymptotic diffusion theory, the two-group numeral example of Section III will be recalculated with use of the previously obtained B-value from diffusion theory in the asymptotic equations:

$$B^2_{D.T.} \cong 0.005 \text{ cm}^{-2}, \quad B_{D.T.} \cong 0.0733 \text{ cm}^{-1}$$

Group I

$$\frac{B^2_{D.T.}}{3\Sigma_I} = 0.00929, \quad \frac{B^2_{D.T.}}{3\Sigma_I}\left(1 - \frac{4}{15}\frac{B^2}{\Sigma_I^2}\right) = 0.00880.$$

Hence, for Group I diffusion theory gives about 4% more leakage in this case.

Group II

$$\frac{B^2_{D.T.}}{3\Sigma_{II}} = 0.00631, \quad \frac{B^2_{D.T.}}{3\Sigma_{II}}\left(1 - \frac{4}{15}\frac{B^2}{\Sigma_{II}^2}\right) = 0.00619.$$

Hence, for Group II diffusion theory gives about 2% more leakage in this case.

The calculated asymptotic diffusion group fluxes are $\overline{\phi}_1 = 5.09$ and $\overline{\phi}_2 = 40.1$. Also, $k_{eff} = 1.011$ with the assumed $B_{D.T.} = 0.0733 \text{ cm}^{-1}$. Comparison with $k_{eff}^{D.T.} = 1.005$, obtained with use of the same buckling, shows that the result of diffusion theory corresponds to about 0.6% less reactivity than is obtained by the asymptotic method.

It may be noted that the normal-mode, many-group ELMOE[30] and GAM[26] codes, whose group intervals are quite narrow, contain consistent B_1 options which allow for linear scattering, including anisotropic scattering to other groups.

Use of normal-mode calculations arises also in connection with the calculation of reflector savings. The difference of reflected core radius and extrapolated bare core radius derived from asymptotic-theory material-buckling calculations, for consistency, should be based upon, for example, a DSN reflected core calculation having a sufficiently high-order angular flux approximation. The scattering anisotropy in both the normal-mode and the DSN calculation should be equivalent, i.e., both isotropic or both linearly anisotropic, employing the transport approximation.

X. EQUILIBRIUM SPECTRUM AND FAST DIFFUSION LENGTH

Comparison of calculated integral quantities with corresponding experimental measurements is one means of checking in a gross manner the validity of a multigroup cross-section set. Some integral measurements are critical mass, detector foil activations, fission detector rates, reactivity effects of material replacements both local and uniform, and prompt-neutron lifetime.(8,41)

As an example of a comparison of calculation with experiment, a choice of particular interest, both from the point of view of a check on U^{238} cross sections and because it represents integral measurements on a system having $k_\infty < 1$, is the Snell block experiment.(42) Analytically, it illustrates also the use of normal-mode calculation for negative B^2.

The Snell experiment consists of a very large block of natural uranium into one face of which neutrons diffuse from a source such as a reactor thermal column. Within some distance into the block the initial neutrons are essentially absorbed. The fission absorptions in the natural uranium block produce fission spectrum sources. The neutrons from the latter sources then undergo the various fission, capture, slowing-down, and diffusion processes as determined by the various cross sections of natural uranium.

At a sufficiently large distance into the block the flux spectrum becomes independent of position. The fission source distribution and the flux distribution in space are such then of the form e^{iBx}, where B is imaginary, i.e., $e^{-|B|x}$, assuming that block is of infinite extent in the radial directions. The spectrum is then referred to as an equilibrium spectrum, and $L \equiv 1/|B|$ is called the fast diffusion or relaxation length.

Measured relative responses of various detectors allow estimates of the equilibrium spectrum. Traverses of detectors through regions of the block having the equilibrium spectrum enable measurement of the fast diffusion length.

From the point of view of fast reactor physics the comparison of measured and calculated values of fast diffusion length is instructive. It is a quantity especially sensitive to the transport and capture cross sections, as well as to the inelastic-scattering matrix.

Measurements with depleted uranium have been reported by Russian investigators.(43)

In a natural uranium blanket surrounding a reactor core the flux spectrum approaches equilibrium at large distances from the core. Experiments of this type have been reported by the British for the blanket of the fast reactor Zephyr.(44)

With a spatial distribution of the form $e^{-|B|x}$, the multigroup normal-mode analysis may be used. Either the group leakage term $-|B^2|/3\Sigma_{tr_j}$ or the more accurate leakage term of the B_0 method with transport approximation,

$$\left[\frac{|B|}{\tanh^{-1}(|B|/\Sigma_{tr_j})} - \Sigma_{tr_j}\right],$$

is used. The successive group fluxes are calculated, followed by iteration by varying $|B|$ until convergence. Convergence in this case is determined when the relative levels of the group fluxes are such that the neutron flow into a unit volume plus the fission sources produced in the unit volume equals the total absorptions in the unit volume.

A recently reported measurement of relaxation length, 9.17 ± 0.18 cm, is that of Chezem.[42] An Oak Ridge value[45] is 9.6 cm and an Argonne measurement[46] has given 10.0 ± 0.2 cm.

Yiftah et al.,[23] have calculated a value of 8.86 cm, which is low relative to the experimental values, as is also a previously calculated value of 8.5 cm by Meneghetti et al.[47]

It is instructive to note that the latter investigators obtained previously the calculated value of 9.9 cm. Availability of newer inelastic scattering data, however, resulted in the subsequently calculated lower value of 8.5 cm. This illustrates an example of the sensitivity, in certain cases, of integral quantities to cross-section parameters. In this case, it shows the sensitivity of L to the inelastic-scattering matrix.

XI. RESONANCE SCATTERING EFFECTS ON GROUP PARAMETERS

In averaging cross sections over the energy interval of a group, some assumption is made as to the $\phi(E)$ within the group. Generally, at very high energies this is assumed to be a fission source distribution. At energies on the high side of the flux maximum and on the low side of the flux maximum, suitable smooth decreasing and increasing functions of energy are used. In the energy region of the maximum, a constant flux weight is often assumed. After an initial calculation a smooth curve may be drawn through the flux-distribution histogram obtained from the group fluxes to obtain an improved gross spectral shape for intragroup weightings.

If a large number of groups having very small group intervals are used, the question of the intragroup flux distribution generally becomes unimportant. The group widths $(\Delta E)_j$, however, are not generally chosen to be so small that the elastic-scattering moderation into lower groups than into the adjacent lowest group need be considered. This restriction reduces considerably the parameters required. If the heavy fuel and fertile materials are the predominant materials in the system, this restriction introduces negligible error.

If considerable amounts of intermediate and lighter materials are present, such as the common diluents and structural materials: iron, sodium, and aluminum, this restriction can introduce errors if a priori improved intragroup $\phi_j(E)$ are not used in the weighted averaging of the group cross sections.[30] This difficulty does not arise because of the greater moderating effect, but because of the prominent resonance scattering characteristics of these materials in the fast energy range from a few kilovolts to the MeV region, especially below ~0.5 MeV. The evaluations of group-transport and group elastic-transfer cross sections must consider these detailed resonances.

Consider that the group energy interval ΔE_j contains resonances. As an idealization, consider that the energy region of interest is sufficiently removed from the Placzek function effects due to fission and inelastic scattering sources at higher energies. The cross section in the group is assumed to be that of pure elastic scattering. As

$$\left(\frac{\bar{1}}{\sigma_{tr}}\right)_j = \int_{\Delta E_j} \frac{\phi(E)}{\sigma_{tr}(E)}\, dE \Big/ \int_{\Delta E_j} \phi(E)\, dE$$

where

$$\sigma_{tr}(E) = \sigma_s(E)(1 - \bar{\mu})$$

and as the collision density is constant per unit lethargy,

$$E\phi(E)\sigma_S(E) = \text{const.},$$

so that

$$\phi(E) = \frac{\text{const.}}{E\sigma_S(E)},$$

then

$$\left(\frac{\bar{l}}{\sigma_{tr}}\right)_j = \int_{\Delta E_j} \frac{dE}{E\sigma_S^2(E)[1-\bar{\mu}(E)]} \Bigg/ \int_{\Delta E_j} \frac{dE}{E\sigma_S(E)}.$$

Now, in a fast reactor the envelope of the low-energy side of the spectral distribution does not vary as $1/E$; in fact, neglecting the fine flux variations due to resonances, the envelope decreases with decreasing energy. If the group increment ΔE_j is, however, not large relative to the smoothed-out envelope, but large compared with the widths of resonances within ΔE_j, then the envelope variation is negligible and

$$\left(\frac{\bar{l}}{\sigma_{tr}}\right)_j \cong \int_{\Delta E_j} \frac{dE}{\sigma_S^2(E)[1-\bar{\mu}(E)]} \Bigg/ \int_{\Delta E_j} \frac{dE}{\sigma_S(E)}$$

The contributions of the resonances to the group transport cross section are diminished due to the diminished flux magnitudes at the resonances.

In practice, not only must other cross sections be considered, but also cross sections of the other materials present, and in particular the resonance cross sections of other scattering materials. Strictly, then, homogenization should precede the averaging evaluation. In general, if resonance effects are not considered in the detailed $\phi(E)$ weighting function within the group, but are considered in the transport cross section $\sigma_{tr}(E)$ within the group, the group transport cross section will tend to be excessive.

Hummel and Rago at Argonne have developed the ELMOE code,[30] an IBM-704 program, in an attempt to carry out proper averages of group cross sections for transport and elastic transfer. (Clearly the positions of resonances relative to the end points of the group interval are important in the evaulations of the transfer of neutrons out of the interval.) They employ many hundreds of very narrow subgroups to cover the whole energy range of interest in the system, including a detailed elastic-scattering matrix and details of resonances. The normal-mode analysis is by the simple diffusion, consistent P_1, or consistent B_1 method.

An example of the effect of detailed resonance consideration on values of group cross sections are shown in Table VII. Listed are the ratios

of ELMOE-modified to unmodified Yiftah et al.,[23] cross sections for aluminum in a predominantly aluminum diluent critical assembly and for stainless steel in a stainless steel diluent critical assembly.[48]

Table VII

RATIO OF MODIFIED TO UNMODIFIED CROSS SECTIONS FOR ALUMINUM AND FOR STAINLESS STEEL

(From Ref. 48)

Energy Group	Lower Energy of Group (MeV)	Ratio			
		Aluminum		Stainless Steel	
		Transport	Elastic Transfer	Transport	Elastic Transfer
1	3.668	(1)[a]	(1)	(1)	(1)
2	2.225	0.83	1.11	0.86	0.81
3	1.35	0.95	1.25	0.97	1.14
4	0.825	0.85	1.02	0.91	1.03
5	0.5	0.945	1.11	0.95	1.11
6	0.3	0.94	1.02	0.86	0.78
7	0.18	0.76	0.93	0.94	1.03
8	0.11	0.61	0.84	0.84	0.99
9	0.67	0.475	0.61	0.64	0.80
10	0.0407	0.67	0.68	0.95	0.95
11	0.025	0.24	0.36	0.49	0.75
12	0.015	1.07	1.00	0.67	0.73
13	0.0091	0.97	1.00	0.98	0.98
14	0.0055	(1)	(1)	(1)	(1)
15	0.0021	(1)	(1)	(1)	(1)
16	0.0005	(1)	(1)	(1)	(1)

[a]Indicates no ELMOE calculation for these groups.

In a calculational study[48] of a series of ZPR-III fast critical assemblies, Meneghetti concluded that use of the simple P-1 ELMOE-averaging corrections leads to critical mass values ~5 to 10% greater than those calculated from the direct, Yiftah et al., set of cross sections.

As the ELMOE code is a fundamental-mode analysis, the question of resonance effects in the outer region of a core and in a blanket region is not, however, directly resolved.

Assuming that the transport cross section is properly resonance averaged, the following trends given by Hummel and Rago[30] illustrate the effects of interrelation of cross sections:

(a) The presence of increasing amounts of U^{235} and U^{238} tends to increase effective transport cross sections, since these elements add a constant transport cross section to a mixture which fills in low places in the resonance scattering cross sections. Such regions have a high weight in the $1/\Sigma_{tr}$ averaging process because of flux rise at these points.

(b) Increasing amounts of a single light element tend to decrease the transport cross section of that element for the same reason.

(c) A mixture of light elements tends to lead to higher apparent transport cross sections for the individual elements, because the minima in the cross section of a given element are usually filled in by other elements.

XII. MULTIGROUP ADJOINT FLUX AND PERTURBATION ANALYSIS

Although familiarity with the adjoint concept is assumed, a brief review with emphasis on the multigroup formulation will be presented. The adjoint fluxes can enter into calculation of quantities such as effective delayed-neutron fraction, neutron lifetime, reactor period, and material-replacement effects. Calculation of these quantities in fast reactor analyses is generally by multigroup methods. The comparisons of results of calculations of these integral quantities with experimental results judge the reliability of cross-section parameters, methods of calculations, and, at times, even the reliability of experimental data.

The N-energy group diffusion equation with downward transfer coefficients may be written (for example, see Ref 8) as

$$D_j \nabla^2 \phi_j - \sigma_{a_j} \phi_j - \sigma_{j\rightarrow} \phi_j + \chi_j \sum_{k=1}^{N} (\nu\sigma_f)_k \phi_k + \sum_{k=1}^{k=j-1} \sigma_{k\rightarrow j} \phi_k = 0;$$

$$j = 1,\ldots,N,$$

where σ_{a_j} is the sum of group capture and fission cross sections, $\sigma_{j\rightarrow}$ is the transfer cross section out of the group, $\sigma_{k\rightarrow j}$ is the transfer cross section from group k to group j, and χ_j is the fraction of the fission spectrum in group j (assumed identical for all fissionable isotopes). The σ's are here to be understood as homogenized, microscopic cross sections.

As is known, the set of equations may be expressed as a matrix equation $(M)(\phi) = 0$ where (ϕ) is the column vector consisting of the components ϕ_j. The corresponding adjoint equation for the adjoint flux, $(M^+)(\phi^+) = 0$, is directly obtainable by interchange of rows and columns of (M) to form (M^+).[49]

Thus, with two groups,

$$D_1 \nabla^2 \phi_1 - \sigma_{a_1} \phi_1 - \sigma_{1\rightarrow 2} \phi_1 + \chi_1 (\nu\sigma_f)_1 \phi_1 + \chi_1 (\nu\sigma_f)_2 \phi_2 = 0$$

and

$$D_2 \nabla^2 \phi_2 - \sigma_{a_2} \phi_2 + \chi_1 (\nu\sigma_f)_1 \phi_1 + \chi_2 (\nu\sigma_f)_2 \phi_2 + \sigma_{1\rightarrow 2} \phi_1 = 0$$

may be written in matrix form as

$$\begin{pmatrix} (D_1\nabla_1^2 - \sigma_{a_1} - \sigma_{1\to 2} + \chi_1 \nu\sigma_{f_1}) & (\chi_1 \nu\sigma_{f_2}) \\ (\chi_2 \nu\sigma_{f_1} + \sigma_{1\to 2}) & (D_2\nabla_2^2 - \sigma_{a_2} + \chi_2 \nu\sigma_{f_2}) \end{pmatrix} \begin{pmatrix} \phi_1 \\ \phi_2 \end{pmatrix} = 0.$$

The matrix adjoint, (M^+), is then

$$(M^+) \equiv \begin{pmatrix} (D_1\nabla_1^2 - \sigma_{a_1} - \sigma_{1\to 2} + \chi_1 \nu\sigma_{f_1}) & (\chi_2 \nu\sigma_{f_1} + \sigma_{1\to 2}) \\ (\chi_1 \nu\sigma_{f_2}) & (D_2\nabla_2^2 - \sigma_{a_2} + \chi_2 \nu\sigma_{f_2}) \end{pmatrix},$$

and the adjoint equations are

$$D_1\nabla^2\phi_1^+ - \sigma_{a_1}\phi_1^+ - \sigma_{1\to 2}\phi_1^+ + \chi_1 \nu\sigma_{f_1}\phi_1^+ + \chi_2 \nu\sigma_{f_1}\phi_2^+ + \sigma_{1\to 2}\phi_2^+ = 0$$

and

$$D_2\nabla^2\phi_2^+ - \sigma_{a_2}\phi_2^+ + \chi_2 \nu\sigma_{f_2}\phi_2^+ + \chi_1 \nu\sigma_{f_2}\phi_1^+ = 0.$$

Extension to more energy groups is evident.

In general, then, for a critical system

$$(M)(\phi) = 0; \quad (M^+)(\phi^+) = 0.$$

The matrix (M) may, however, be expressed as the sum of production and loss matrices:

$$(M) \equiv (P) + (L).$$

In two groups, for example,

$$(P) = \begin{pmatrix} (\chi_1 \nu\sigma_{f_1}) & (\chi_1 \nu\sigma_{f_2}) \\ (\chi_2 \nu\sigma_{f_2}) & (\chi_2 \nu\sigma_{f_2}) \end{pmatrix}$$

and

$$(L) = \begin{pmatrix} (D_1\nabla_1^2 - \sigma_{a_1} - \sigma_{1\to 2}) & (0) \\ (\sigma_{1\to 2}) & (D_2\nabla_2^2 - \sigma_2) \end{pmatrix}.$$

For a critical system, then,

$$(P + L)(\phi) = 0.$$

In general, for a critical or noncritical system,

$$\left(\frac{P}{k} + L\right)(\phi) = 0,$$

and

$$k = \frac{(P)(\phi)}{(L)(\phi)}.$$

The (ϕ) are here the solutions with matrices (P) and (L). Also, as $k^+ = k$, the general adjoint equation is

$$\left(\frac{P^+}{k} + L^+\right)(\phi^+) = 0.$$

By use of the flux and adjoint equations, and the adjoint properties

$$\iint (\phi^+)(P)(\phi)\, dV dE = \iint (\phi)(P^+)(\phi^+)\, dV dE$$

and

$$\iint (\phi^+)(L)(\phi)\, dV dE = \iint (\phi)(L^+)(\phi^+)\, dV dE,$$

it may be shown that

$$k = \frac{\iint (\phi^+)(P)(\phi)\, dV dE}{\iint (\phi^+)(L)(\phi)\, dV dE}$$

is stationary. By this equation k' may be estimated for systems having matrix operators (P') and/or (L') differing slightly for (P) and (L) by replacement of the primed matrices for the unprimed in the integrals, the flux and adjoints being known solutions of the unprimed matrix diffusion equations.

The perturbation expression for fractional change in the eigenvalue is then directly obtainable by differentiation (square brackets here represent the integrations) where $(\delta\phi^+)$ and $(\delta\phi)$ are neglected:[49]

$$\frac{\delta k}{k} = \frac{[(\phi^+)(\delta P)(\phi)]}{[(\phi^+)(P)(\phi)]} - \frac{[(\phi^+)(\delta L)(\phi)]}{[(\phi^+)(L)(\phi)]}.$$

This further reduces to

$$\frac{\delta k}{k} = \frac{[(\phi^+)(\delta P - \delta L)(\phi)]}{[(\phi^+)(P)(\phi)]},$$

if k is unity for the unperturbed system. The denominator is the volume-energy integral of importance-weighted fission neutrons in the entire system before the perturbation.

The forms of the integrals for multigroup perturbation analyses may be illustrated by the explicit expressions for two-energy groups. The denominator is then

$$[(\phi^+)(P)(\phi)] = \int \phi_1^+ \chi_1 \nu_1 \sigma_{f_1} \phi_1 \, dV + \int \phi_1^+ \chi_1 \nu_2 \sigma_{f_2} \phi_2 \, dV$$

$$+ \int \phi_2^+ \chi_2 \nu_1 \sigma_{f_1} \phi_1 \, dV + \int \phi_2^+ \chi_2 \nu_2 \sigma_{f_2} \phi_2 \, dV,$$

where the cross sections are macroscopic, the integrals are over the entire volume of the system, and the fluxes and adjoints are the group fluxes and adjoints of the unperturbed system. The numerator terms are

$$[(\phi^+)(\delta P)(\phi)] = \int \phi_1^+ \chi_1 \delta(\nu_1 \sigma_{f_1}) \phi_1 \, dV + \int \phi_1^+ \chi_1 \delta(\nu_2 \sigma_{f_2}) \phi_2 \, dV$$

$$+ \int \phi_2^+ \chi_2 \delta(\nu_1 \sigma_{f_1}) \phi_1 \, dV + \int \phi_2^+ \chi_2 \delta(\nu_2 \sigma_{f_2}) \phi_2 \, dV$$

and

$$-[(\phi^+)(\delta L)(\phi)] = -\int \phi_1^+ \delta\sigma_1 \phi_1 \, dV - \int \phi_2^+ \delta\sigma_2 \phi_2 \, dV - \int \phi_1^+ \delta\sigma_{1\to 2} \phi_1 \, dV$$

$$+ \int \phi_2^+ \delta\sigma_{1\to 2} \phi_1 \, dV - \int \delta D_1 \bar{\nabla} \phi_1^+ \cdot \bar{\nabla} \phi_1 \, dV - \int \delta D_2 \bar{\nabla} \phi_2^+ \cdot \bar{\nabla} \phi_2 \, dV.$$

In the latter expression the first two integrals represent the group absorption (capture plus fission) effects. The third and fourth terms taken together represent the effect of the net difference in importance of neutrons transferred, i.e.,

$$\int (\phi_2^+ - \phi_1^+) \, \delta\sigma_{1\to 2} \phi_1 \, dV.$$

This indicates the physical meaning of the adjoint function. Thus, $\delta\sigma_{1\to 2} \phi_1$ corresponds to a neutron sink or negative source in group 1 and

simultaneously a neutron source in group 2. The importance of this exchange in its effect upon reactivity, and hence upon the overall neutron inventory, is determined by the relative values of the adjoints. Physically then, for example, if a relatively small number of neutrons are continuously externally added or removed at a particular position and energy in a slightly subcritical system, the overall relative flux is proportional to the ϕ^+ at that position and energy. The last two terms give the importance of leakage effects in the perturbed region. These diffusion terms are obtained in the given gradient product form by application of the divergence theorem and the vector relation

$$\overline{\nabla} \cdot (A\overline{\nabla}B) = \overline{\nabla}A \cdot \overline{\nabla}B + A\overline{\nabla}B.$$

It is noted that the leakage effect terms are zero at the reactor center where the gradients are zero. Thus, for central danger coefficient calculations they do not enter the calculation.

It is both useful and instructive to carry out the fundamental-mode analysis for the group adjoint fluxes in analogy with the previous bare core flux analysis. By substituting $-D_1B^2\phi_1^+$ and $-D_2B^2\phi_2^+$ in the two-group adjoint equations for the $D_1\nabla^2\phi_1^+$ and $D_2\nabla^2\phi_2^+$ terms, one obtains, in the reverse order,

$$\phi_2^+ = \frac{(\nu_2\sigma_{f_2})(\chi_1\phi_1^+ + \chi_2\phi_2^+)}{\sigma_{a_2} + D_2B^2}$$

and

$$\phi_1^+ = \frac{(\nu_1\sigma_{f_1})(\chi_1\phi_1^+ + \chi_2\phi_2^+) + \sigma_{1\to 2}\phi_2^+}{\sigma_{a_1} + \sigma_{1\to 2} + D_1B^2}.$$

The eigenvalue is then given by

$$k = \frac{(\chi_1\phi_1^+ + \chi_2\phi_2^+)'}{(\chi_1\phi_1^+ + \chi_2\phi_2^+)},$$

where the denominator is the initially assumed value, which may be taken as unity, thus simplifying the group adjoint expressions.

The equality $k^+ = k$ may be directly shown by substitution of the explicit expressions for ϕ_1^+ and ϕ_2^+ into the above expression for k.

It is of interest to compare some multigroup central danger coefficient calculations by perturbation analysis with experiments. Long et al.,[50] has reported a few comparisons between measurements of fast critical assemblies constructed in the Argonne fast facility ZPR-III and calculated

reactivities. These calculations were made with the 16-group Yiftah et al., set.[23] To avoid calculation of the importance volume integral of fission neutron sources over each of the assemblies, the results were normalized by ad hoc equation of the calculated and experimental values for Pu^{239}. The values listed in Table VIII are given in millibarns and normalized to the effective Pu^{239} cross section per atom in the given fast assembly spectrum calculated by $[(\nu - 1)\sigma_f - \sigma_c]^{Pu^{239}}$.

Table VIII

EXPERIMENTAL AND CALCULATED CENTRAL REACTIVITY COEFFICIENTS (in mb)

(from Ref. 50)

Material	Assembly 22		Assembly 23		Assembly 29	
	Exp	Calc	Exp	Calc	Exp	Calc
Pu^{239}	3238		3395		3250	
U^{235}	1772	1939	1774	1964	1913	2066
U^{238}	-84	-94.8	40	67.5	-100	-97.9
Al	-13.1	-10.4	3.5	12.2	2.2	2.6
Fe	-23.8(SS*)	-24.4	0.9	2.6	-6.7(SS)	-8.5

*SS = Stainless Steel.

The core of Assembly 22 is about 9.4 v/o U^{235}, 70 v/o U^{238}, and 9 v/o stainless steel. Assembly 23 is about 9.3 v/o U^{235}, 0.7 v/o U^{238}, 43 v/o aluminum, and 9 v/o stainless steel. Assembly 29 represents an oxide (UO_2) core having about 5 v/o U^{235}, 10 v/o U^{238}, 24 v/o aluminum, 25 v/o stainless steel, and 14.5 v/o oxygen of density 2.55 gm/cc.

It is seen that U^{238} is positive in the harder spectrum Assembly 23 where fast fission is more important. For materials which are neither strongly capturing nor fissioning, the sign and magnitudes of danger coefficients are very sensitive to the adjoint functions through the group transfer matrices.

XIII. PROMPT-NEUTRON LIFETIME AND EFFECTIVE DELAYED-NEUTRON FRACTION

Another integral quantity of interest is the prompt-neutron lifetime of a system. For a fast system this is many orders of magnitude smaller than for a thermal system. As a consequence, if the reactivity of the system is more than prompt critical, the flux level of the fast system will rise extremely rapidly. For example, for a fast reactor the prompt-neutron lifetime $\ell_p \cong 10^{-7}$ sec, whereas for thermal reactors $\ell_p \cong 10^{-3}$ to 10^{-5} sec.

Recall that the exponential increase in flux level for a system having excess prompt reactivity Δk_p varies with time as $e^{+\alpha t}$, where $\alpha = \Delta k_p/\ell_p$. If, then, the exponential time variation, $\phi = \varphi(x)\, e^{\alpha t}$, is substituted into the time-dependent diffusion equation,

$$D\nabla^2\phi - \Sigma_a\phi + \nu\Sigma_f\phi = \frac{1}{v}\frac{\partial\phi}{\partial t},$$

there is obtained a modified form of spatial equation:

$$D\nabla^2\varphi - \left(\Sigma_a + \frac{\alpha}{v}\right)\varphi + \nu\Sigma_f\varphi = 0.$$

The spatial solution differs from the case of a non-time-dependent case by the effect of the term $(\alpha/v)\varphi$. ℓ_p may be obtained by adding a 1/v-absorber throughout all regions of the system and evaluating the change in k_{eff} due to the 1/v-absorber. If, then, the macroscopic cross section of the 1/v-absorber is c/v, then

$$\ell_p = \Delta k_{calculated}/c.$$

For multigroup analyses the group velocity v_j may be estimated by

$$\frac{1}{v_j} = \frac{\int_{group\ j} \frac{\phi(E)\,dE}{v(E)}}{\int_{group\ j} \phi(E)\,dE},$$

where $\phi(E)$ is some suitable assumed spectral distribution within the group.

Calculation of ℓ_p can also proceed by use of fluxes and adjoint fluxes of the unperturbed system.[49] In this method,

$$\ell_p \iint_{\substack{\text{all}\\ \text{EdV}}} \phi^+ L\phi \, dV dE = \iint_{\substack{\text{all}\\ \text{EdV}}} \frac{\phi^+\phi}{v} \, dV dE,$$

as the lifetime multiplied by the loss rate of importance equals the total importance of all the neutrons, i.e., $\iint \phi^+ N dE dV$, where $N = \phi/v$. As will be illustrated for the case of two energy groups, either ϕ^+ or N^+ may be used in this importance weighting because both satisfy identical form of adjoint diffusion equations.

For a critical system the loss rate of importance equals the production rate of importance, the latter being an easier quantity to calculate. Thus,

$$\ell_p = \frac{\iint \frac{\phi^+\phi}{v} \, dV dE}{\iint \phi^+ P \phi \, dV dE}.$$

The multigroup form of the expression is illustrated by the explicit two-group form:

$$\ell_p = \frac{\int \frac{\phi_1^+\phi_1}{v_1} \, dV + \int \frac{\phi_2^+\phi_2}{v_2} \, dV}{\int (\chi_1 \phi_1^+ \nu_1 \Sigma_{f_1} \phi_1 + \chi_1 \phi_1^+ \nu_2 \Sigma_{f_2} \phi_2 + \chi_2 \phi_2^+ \nu_1 \Sigma_{f_1} \phi_1 + \chi_2 \phi_2^+ \nu_2 \Sigma_{f_2} \phi_2) \, dV},$$

where the volume integrals are over the entire reactor system.

The $1/v$ insertion method results in the same ℓ_p value as obtained by the adjoint weighting method in the limit as $c \to 0$ in a series of $1/v$ calculations. In a $1/v$ insertion calculation, as the amount of absorber inserted is decreased, round-off errors become increasingly important. Satisfactory agreement between the two methods may be obtained, however, by extrapolation of the $1/v$ insertion results for various absorber strengths to zero absorber.

The previous comment upon the equivalence of form of the N^+ and ϕ^+ equations may be illustrated by use of the two-group normal-mode solutions previously described. In terms of

$$v_1 N_1^+ = \phi_1^+ \text{ and } v_2 N_2^+ = \phi_2^+,$$

the matrix equation for (N^+) is

$$\begin{pmatrix} (v_1 D_1 \nabla_1^2 - v_1\sigma_1 - v_1\sigma_{1\to 2} + v_1\chi_1\nu_1\sigma_{f_1}) & (v_1\chi_2\nu_1\sigma_{f_1} + v_1\sigma_{1\to 2}) \\ (v_2\chi_1\nu_2\sigma_{f_2}) & (v_2 D_2\nabla_2^2 - v_2\sigma_2 + v_2\chi_2\nu_2\sigma_{f_2}) \end{pmatrix} \begin{pmatrix} N_1^+ \\ N_2^+ \end{pmatrix} = 0.$$

If the Laplacians are replaced by the buckling B^2, the equations

$$-v_1 D_1 B^2 N_1^+ - v_1\sigma_1 N_1^+ - v_1\sigma_{1\to 2} N_1^+ + v_1\chi_1\nu_1\sigma_{f_1} N_1^+ + v_1\chi_2\nu_1\sigma_{f_1} N_2^+ + v_1\sigma_{1\to 2} N_2^+ = 0$$

and

$$+v_2\chi_1\nu_2\sigma_{f_2} N_1^+ - v_2 D_2 B^2 N_2^+ - v_2\sigma_2 N_2^+ + v_2\chi_2\nu_2\sigma_{f_2} N_2^+ = 0$$

then allow the normal-mode solutions for the N^+ to be obtained:

$$N_2^+ = \frac{v_2\nu_2\sigma_{f_2}[\chi_1 N_1^+ + \chi_2 N_2^+]}{v_2\sigma_2 + v_2 D_2 B^2};$$

$$N_1^+ = \frac{v_1\nu_1\sigma_{f_1}[\chi_1 N_1^+ + \chi_2 N_2^+] + v_1\sigma_{1\to 2} N_2^+}{v_1\sigma_1 + v_1\sigma_{1\to 2} + v_1 D_1 B^2}.$$

As the group velocities cancel out, it is seen that the form of the equations are identical with the ϕ_2^+ and ϕ_1^+ equations obtained in previous discussions.

The quantity β_{eff}, the effective delayed-neutron fraction, may also be calculated by use of the group flux and adjoint solutions of the diffusion equations.[48,49] β_{eff} is given by $\beta_{eff} = D/(P+D)$, where D is a quantity proportional to the worth of all the delayed neutrons and P is a quantity proportional to the worth of all prompt neutrons.

In the multigroup notation and for the case of, for example, the fissionable species U^{235} and U^{238}, D and P have the explicit forms:

$$D = \beta^{25} \int_V \left[\sum_j (\nu\sigma_f)_j^{25} \phi_j\right]\left[\sum_j \chi_j^{25D} \phi_j^+\right] dV$$

$$+ \beta^{28} \int_V \left[\sum_j (\nu\sigma_f)_j^{28} \phi_j\right]\left[\sum_j \chi_j^{28D} \phi_j^+\right] dV$$

and

$$P = [1 - \beta^{25}] \int_V \left[\sum_j (\nu\sigma_f)_j^{25} \phi_j\right]\left[\sum_j \chi_j \phi_j^+\right] dV$$

$$+ [1 - \beta^{28}] \int_V \left[\sum_j (\nu\sigma_f)_j^{28} \phi_j\right]\left[\sum_j \chi_j \phi_j^+\right] dV.$$

The fission fractions of the delayed and prompt neutrons are normalized separately by

$$\sum_j \chi_j^{25D} = 1; \quad \sum_j \chi_j^{28D} = 1; \quad \sum_j \chi_j = 1.$$

The β^{25} and β^{28} of the individual fissionable species may be evaluated from experimental values of (n/F), the number of delayed neutrons per fission, and of $\overline{\nu}$, the mean value of the number of total neutrons emitted per fission, by the equation

$$\beta = \frac{1}{\overline{\nu}}\left(\frac{n}{F}\right)$$

for each species. For example, some listed experimental values for the case of fast neutron fission are:[51,52]

$$\left(\frac{n}{F}\right)^{25} = 0.0165; \quad \overline{\nu}^{25} = 2.56;$$

$$\left(\frac{n}{F}\right)^{28} = 0.0412; \quad \overline{\nu}^{28} = 2.62.$$

The delayed-neutron fraction for U^{238} is seen to be much larger than that of U^{235}. For comparison, other (n/F) values are 0.0063, 0.0070, and 0.0496 for Pu^{239}, U^{233}, and Th, respectively.[52]

The spectra of delayed neutrons have mean energies considerably lower than the ~2 MeV of the prompt-neutron spectra. The reported[53] mean energies of the delayed neutrons of U^{235}, for example, are about 250 to 900 keV, depending upon the particular delayed period. Attempts have been made to obtain the detailed delayed spectra for the particular delayed groups[54] as well as a detailed, averaged delayed spectrum.[53]

As a fast system often contains large quantities of, for example, fertile U^{238} material in both core and breeder blanket, the neutron spectrum

of a fast reactor is such that a considerable fraction of the fissions occur in the U^{238}. The calculation of β_{eff}, and as will be seen later of the reactivity-period relationships, are dependent upon the relative spatial distributions of the fertile and fuel fissions.

Illustrative of multigroup (10 groups) calculations of ℓ_p and β_{eff} by the adjoint methods compared with experimental values of

$$\alpha_R^{exp} = (\beta_{eff}/\ell_p)_{exp}$$

are those for a series of zero-power fast assemblies constructed with the Argonne ZPR-III facility[48] as given in Table IX. The measurements[55,50] were by the method of Rossi-α. The observed consistent discrepancy between α_R^{calc} and α_R^{exp} points to as yet-not-understood errors in calculation, experiment, or both.

Table IX

COMPARISON OF CALCULATED AND EXPERIMENTAL VALUES OF (β_{eff}/ℓ_p)

(Based on Table in Ref. 48)

Assembly Number	Calc $\frac{28}{25}$ Fissions		β_{eff}^{calc}	ℓ_p^{calc} x 10^8 sec	$\alpha_R^{calc} = \frac{\beta_{eff}^{calc}}{\ell_p^{calc}}$, sec^{-1} x 10^{-5}	α_R^{exp}, sec^{-1} x 10^{-5}
	In Core	Total				
6F	0.08	0.27	0.00734	6.57	1.12	0.985
9A	0.17	0.31	0.00739	6.39	1.16	-
22 (or 11)	0.305	0.38	0.00731	5.77	1.27	1.04
24	0.35	0.42	0.00726	6.64	1.09	0.851
25	0.35	0.40	0.00718	6.77	1.06	0.91

The value of β_{eff} may also be calculated without using adjoint functions. In this seemingly more direct method,[57] the difference k_{eff} between criticality calculations with and without the delayed neutrons is obtained. This gives directly $\beta_{eff} = \Delta k_{eff}$. The prompt spectrum for each material in each group is modified in the second calculation from χ_j^m to $(\chi_j^m - a_j^m \beta^m)$, where a_j^m is the relative abundance of delayed fission neutrons emitted into energy interval of group j by material m and β^m is the total delayed-neutron fraction of material m. Use of this method requires machine criticality codes in which different fission spectra can be used for each isotope. If the code requires that the $\chi^m = \sum_j \chi_j^m = 1$, then the quantity $\sum_j (\chi_j^m - a_j^m \beta^m)$ should be re-normalized for each material and, in addition, all the ν_j^m for all groups of material m should be multiplied by $(1 - \beta^m)$.

It is to be noted that if delayed neutrons of energies near to or lower than the assumed lower limit of the prompt spectrum are being considered in the analysis, then the first problem calculated should contain the fission spectra distribution of both the prompt and delayed neutrons for each isotope; otherwise $(\chi_j^m - a_j^m \beta^m)$ may be negative for the lower groups.

XIV. PERIOD-REACTIVITY RELATIONS

Material-replacement data are frequently reported in units of cents/mole or Ih/kg. A cent is 1/100 of a dollar, $\beta_{eff}/100$, where β_{eff} is the reactivity required to bring a system from delayed critical to prompt critical. An inhour is the reactivity required to attain a stable period of one hour.

For expressing experimental period measurements in such units, it is necessary to relate these units to the measured reactor periods. Similarly, experimental quantities expressed in these units must often be compared with corresponding calculated quantities by use of basic cross-section and delayed-neutron information. The former can be accomplished by calculation of the inhour versus period curve. The latter may be compared by calculation of a factor such as the number of inhours per percent $\Delta k/k$.

For small reactivities and two fissionable species, for example U^{235} and U^{238}, the relation between reactivity and asymptotic period is

$$\rho \cong \sum_{i=1}^{6} \frac{\beta^{25}_{eff_i}}{1 + \lambda^{25} T} + \sum_{i=1}^{6} \frac{\beta^{28}_{eff_i}}{1 + \lambda^{28}_i T},$$

where λ^{25}_i and λ^{28}_i are the decay constants of the i'th decay groups. These decay constants are often taken to be equal; $\lambda^{25}_i = \lambda^{28}_i$. If it is assumed that the delayed-neutron spectra of the delayed groups for a given fissionable species are the same, then[48,55]

$$\beta^{25}_{eff_i} = \frac{D^{25}}{P + D} a^{25}_i,$$

where P and D are as previously defined for the total β_{eff} calculation, D^{25} is the portion of D due to the delayed neutrons of U^{235}, and a^{25}_i is the fraction of the delayed neutrons from U^{235} fission which is emitted into the i'th delayed group having decay constant λ^{25}_i. Analogously,

$$\beta^{28}_{eff_i} = \frac{D^{28}}{P + D} a^{28}_i.$$

If spectral differences in decay groups are to be accounted for, then P, D, etc., must be redefined. Information on detailed delay spectra of the decay groups is quite limited at present. Composite curves or mean energy values are therefore often used.

The ratio $\rho(T)/\beta_{eff}$ gives the reactivities in dollars versus period in seconds, and $\rho(T)/\rho(3600)$ gives the reactivities in inhour units versus period in seconds.

Examples of reactivity-period curves for fast systems are those calculated[48] for a series of fast critical assemblies fueled by U^{235} and having U^{238} as an important diluent contributor (see Fig. 11). The curves are for the range of the usual period measurements in material-replacement experiments. The sensitivity of the curve positions to the composition ratio is evident. This sensitivity also implies a sensitivity to choice of cross-section parameters used in such calculations.

Because the curves of inhour versus period equate the above curves at T = 3600 sec, the resulting inhour-period curves in the reported study of the fast assemblies were found to closely overlap in this range of period, as seen in Fig. 12. This would indicate that the reporting of data in inhours should remove much of the uncertainties that affect the value of an experimentally reported reactivity that result from use of cross-section calculational parameters.

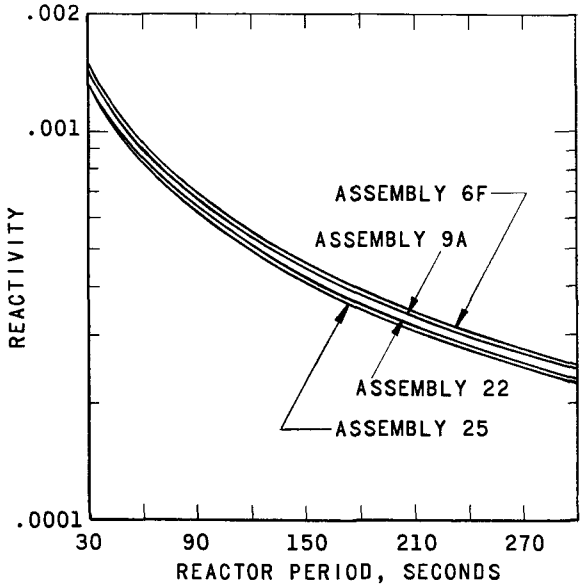

Fig. 11. Curves of Reactivity versus Period for a Series of U^{235}-fueled Fast Assemblies (From Ref. 48)

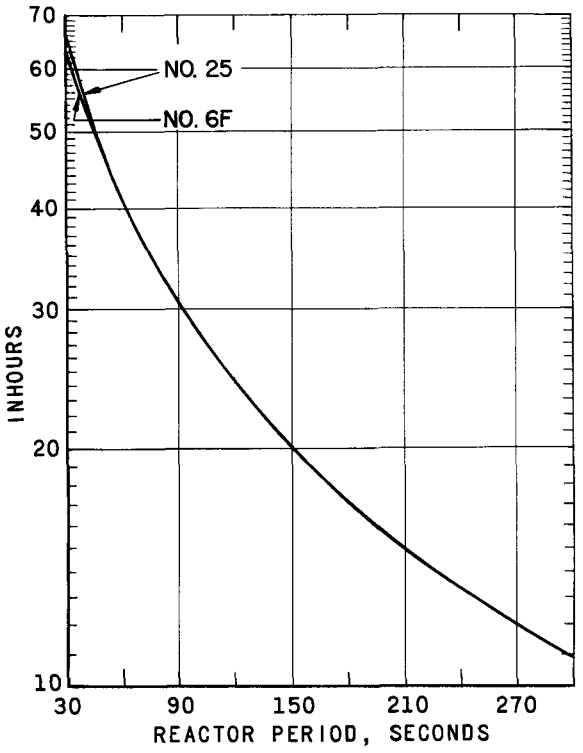

Fig. 12. Curves of Inhour versus Period for a Series of U^{235}-fueled Fast Assemblies (From Ref. 48)

Comparison of experimental reactivity data with calculations necessitate the conversion of inhour to percent $\Delta k/k$. This factor is obtained from the calculated value of $\rho(T = 3600)$:

$$\rho(3600) \cong \sum_{i=1}^{6} \left[\frac{\beta^{25}_{\text{eff}_i} + \beta^{28}_{\text{eff}_i}}{1 + \lambda_i\, 3600} \right] \equiv \frac{\Delta k}{k} \text{ per inhour,}$$

from which

$$\text{inhours}/\%\ \Delta k/k = \frac{1}{\rho(3600)}.$$

As examples are the ih/% $\Delta k/k$ factors calculated for the ZPR-III fast assemblies 6F, 22, and 25. These have been reported[48] as 433, 468, and 481, respectively, on the basis of use of a particular multigroup cross-section set. For comparison, calculations with a somewhat different multigroup set gave values of 425, 458, and 468, respectively, indicating the sensitivity of this factor to cross sections. It is interesting to note that the use of the separate λ_i values for U^{235} and U^{238} are reported to increase these factors by 5 to 10 ih/% $\Delta k/k$. This appears to be caused by the fact that for those delayed groups having the λ_i of the two species most different the abundance is greatest.

XV. SHAPE FACTOR

Criticality calculations by one-dimensional analyses for other than infinite slabs, spheres, and infinite cylinders cannot be carried out because the dimensional separation of the spatial variables is not possible. Furthermore, for the case of, for example, a radially reflected finite cylinder, the axial leakage effects upon reactivity can be accounted for by introducing the equivalent absorption,

$$D_{r,j} B_z^2 \equiv D_{r,j} \frac{\pi^2}{H_z^2},$$

in all regions. Here $D_{r,j}$ is the diffusion constant of region r and group j, the extrapolated bare height of the cylinder is H_z, and B_z^2 is the axial buckling. In most cylindrical systems, however, the presence of axial blankets or reflectors necessitates either an a priori calculated or estimated reflector saving or more directly a two-dimensional R-Z coordinate analysis.

Two-dimensional multigroup analyses, although desirable, are costly and time-consuming, even with fast computing machines, if sufficient number of energy groups, as are often necessary properly to characterize the fast cross sections, are used.

Because fully blanketed cylindrical cores of interest usually have a core height-to-diameter (L/D) ratio neither extremely large nor small, the system corresponds more closely in reflector effects and in reaction rates to an analogous reflected spherical core rather than to a one-dimensional cylinder with axial reflector savings.

In order to estimate a cylindrical critical size from calculations of a spherical system having equal reflector thickness and identical core and reflector compositions, shape factor curves or auxiliary shape factor calculations are necessary. The shape factor may be defined as

$$\text{S.F.} = \frac{\text{Volume of the spherical critical core}}{\text{Volume of the cylindrical core of interest}}.$$

As this is a geometrical correction, it is not necessary, in general, to calculate the shape factor with the use of many energy groups. For most fast systems two or three energy groups should suffice if the few-group cross sections are obtained by group reduction based on weighting of a many-group flux solution. Thus, results of few-group, one-dimensional sphere and analogous two-dimensional cylinder calculation should enable the shape factor to be obtained. The few-group shape factor can subsequently be used to obtain an estimate of a many-group two-dimensional core size by use of the calculated many-group sphere system.

Shape factor curves for various bare and reflected systems based upon experimental data, have been published.(8) Shape factor curves have shapes approximately as sketched in Fig. 13. For a given core composition the shape factor of a reflected system is in general larger than that for the corresponding bare system. As core sizes decrease, the shape factors generally also decrease.

The studies of Loewenstein and Main(58,59) discuss in detail the results of various calculations and approximations.

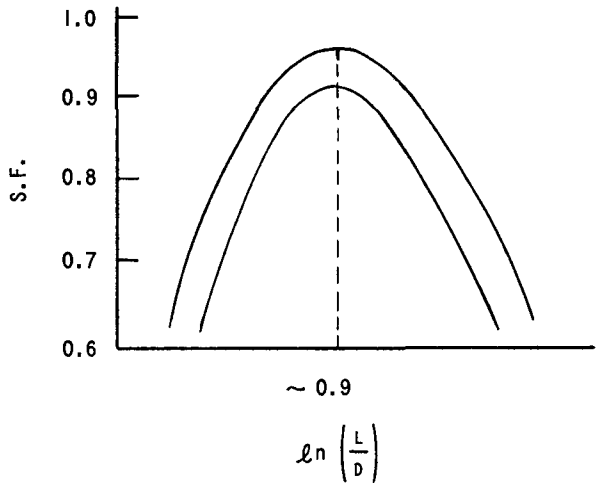

Fig. 13

Sketch of the General Shapes of Shape Factor Curves

XVI. FAST-THERMAL COUPLED SYSTEMS

Before discussing reactivity-temperature effects in fast reactors, the physics calculation aspects of coupled fast-thermal systems will be briefly presented. Interest in coupled systems is due to the possibility of studying fast reactor properties without construction of a large-inventory, short-prompt-lifetime, all-fast critical and to the possibility of using coupled fast power breeders to combine the high breeding ratios of fast reactors with the long neutron lifetime of thermal reactors.

The general coupling theory formulation has been developed by Avery.[60] In the overall reactor system k_{eff} is defined as the average number of fission neutrons in the next generation resulting from a single fission neutron. If one considers the critical system to be composed of, for example, two subcritical parts (in terms of spatial regions or energy divisions), then four integral parameters may be defined: k_1, k_2, k_{12}, and k_{21}. Here k_1 is the average number of next-generation fission neutrons in division 1 resulting from a single fission neutron in division 1, and k_2 is the average number of next-generation fission neutrons in division 2 resulting from a single fission neutron in division 2. We may then define $\Delta_1 \equiv 1 - k_1$ and $\Delta_2 \equiv 1 - k_2$ as the subcriticalities of the respective divisions if for each division the other division is considered solely as a form of reflector with the absorption and scattering properties but with $\nu = 0$. The remaining two integral parameters are a measure of the coupling: k_{12} is the average number of next-generation fission neutrons in division 2 resulting from a single fission neutron in division 1, and analogously, k_{21} is the average number of next generation fission neutrons in assembly 1 resulting from a single fission neutron in Assembly 2.

Then, if S_1 and S_2 are the relative numbers of fission neutron sources in divisions 1 and 2, respectively, the overall criticality conditions of the system in terms of the above integral parameters follow from the requirement that the following equations must be simultaneously satisfied:

$$S_1 = k_1 S_1 + k_{21} S_2$$

and

$$S_2 = k_2 S_2 + k_{12} S_1.$$

Hence, as

$$\begin{vmatrix} (k_{11} - 1) & k_{12} \\ k_{21} & (k_{22} - 1) \end{vmatrix} = 0$$

the critical condition is

$$k_{12} k_{21} = \Delta_1 \Delta_2.$$

At criticality the ratio of the fission neutron sources in the two divisions is

$$\frac{S_1}{S_2} = \frac{k_{21}}{\Delta_1} = \frac{\Delta_2}{k_{12}}.$$

If, then, the division is, for example, between predominantly fast fission and thermal fission spatial regions,

$$\frac{S_F}{S_S} = \frac{k_{SF}}{\Delta_F} = \frac{\Delta_S}{k_{FS}}.$$

The ratio S_F/S_S thus may be increased and Δ_F kept sufficiently large by increasing the coupling from slow to fast regions

A quantity of interest is the division of reactivity Consider the system to be critical. Suppose then that ν_1, the number of neutrons per fission emitted in 1, to be changed by the fraction $\delta\nu_1/\nu_1$. Then the ratio

$$\frac{\delta k}{k} \Big/ \frac{\delta \nu_1}{\nu_1} = \alpha_1,$$

is defined as the fraction of the reactivity in division 1, and analogously for the other division. Correspondingly, α_1 may also be defined through the use of fluxes and adjoint fluxes as

$$\alpha_1 = \frac{\int_{V_1} \int_E \chi\phi^+\nu\Sigma_f\phi dE dV}{\int_V \int_E \chi\phi^+\nu\Sigma_f\phi dE dV}.$$

In terms of the coupling parameters it has been shown that

$$\alpha_1 = \frac{\Delta_2}{\Delta_1 + \Delta_2} \text{ and } \alpha_2 = \frac{\Delta_1}{\Delta_1 + \Delta_2}$$

The prompt-neutron lifetime has also been shown to be expressible as

$$\ell = \frac{\Delta_2 k_1}{\Delta_1 + \Delta_2}\ \ell_1 + \frac{\Delta_1 k_2}{\Delta_1 + \Delta_2}\ \ell_2 + \frac{\Delta_1 \Delta_2}{\Delta_1 + \Delta_2}\ (\ell_{2\to1} + \ell_{1\to2}),$$

where $\ell_{1\to2}$ is defined as the average prompt-neutron lifetime for the process of a fission neutron in division 1 giving rise to a next-generation fission neutron in Assembly 2, etc If, in particular, division 1 signifies a fast fission spatial region and division 2 a thermal fission spatial region, then ℓ_1 and $\ell_{2\to1}$ are very small relative to ℓ_2 and $\ell_{1\to2}$, because the former two parameters do not contain slowing-down times. Then

$$\ell \cong \frac{\Delta_1 k_1}{\Delta_1 + \Delta_2} \ell_2 + \frac{\Delta_1 \Delta_2}{\Delta_1 + \Delta_2} \ell_{1\to 2},$$

which can be further simplified by noting that $\ell_{1\to 2} \cong \ell_2$, so that

$$\ell \cong \frac{\Delta_1}{\Delta_1 + \Delta_2} \ell_2 = \alpha_2 \ell_2.$$

From this it is noted that the prompt-neutron lifetime is then approximately equal to the prompt lifetime of the thermal part multiplied by the fraction of reactivity in the thermal part.

It is instructive to point out some methods of calculations[61] of the various integral parameters by means of multigroup criticality codes. They illustrate examples of how criticality codes may be used to determine quantities other than criticality conditions.

The α_i for each of the i'th division, be it energy-wise and/or geometrical, may be obtained by calculation of δk_{eff} from criticality by variation of the ν_i by a fraction $\delta\nu_i/\nu_i$.

Then

$$\alpha_i = \frac{\delta k_{eff}}{\delta \nu_i/\nu_i}$$

and

$$\sum_i \alpha_i = 1$$

in the limit that all $\delta\nu_i/\nu_i$ approach zero.

The $k_{i\to j}$ may be obtained by use of the multigroup fluxes from a coupled critical calculation. From these fluxes the sources due to fissions in division i are then known. Then use these i'th division sources as applied sources in an inhomogeneous ($\nu = 0$) calculation. From the resulting calculated flux integrals over regions and groups together with the known values of ($\nu\Sigma_f$) of the j'th division, the ratio of the sources is

$$S_{i\to j}/S_i = k_{i\to j}.$$

Analogously,

$$S_{i\to i}/S_i = k_i.$$

Examples for which coupling analyses are useful are schematically a fast fueled region having a filter (decoupling) region separating it from

either a surrounding thermal fueled or thermal moderating region. The Argonne ZPR-V critical assembly[62] and the Atomics International critical[63] for the Advance Epithermal Thorium Reactor Program contained thermal fueled regions surrounding the filters. The Argonne coupled fast breeder critical experiment[61] instead had thermal moderating region surrounding the filter.

Although the coupled systems are only a very particular form of a fast reactor, a brief qualitative discussion of the neutronics will be given because the complexity of the interrelation of the fast, intermediate, and thermal neutrons is instructive in understanding various aspects of fast reactor neutronics in general.

In the coupled power breeder experiment,[61] the central fast core region contained about 14 v/o U^{238}, 15 v/o U^{238}, and 41 v/o aluminum (to simulate sodium coolant). The surrounding filter of natural uranium was about 5 cm thick. The surrounding outer thermal moderator consisted of 27-cm-thick beryllium surrounded by a depleted uranium blanket to capture neutrons otherwise lost by leakage. Qualitatively, for this system the natural uranium functions as a barrier for the thermal and epicadmium resonance region neutrons from going from the beryllium moderator to the fast core. Simultaneously, the filter allows fast core neutrons to traverse the filter and enter the beryllium region to become moderated. Furthermore, because the beryllium region is unfueled, the fuel for the thermalized neutrons is the U^{235} present in the adjacent natural uranium filter. In this experiment $\alpha_{fast} \cong 0.96$, $\alpha_{thermal} \cong 0.04$, and $\ell_p \cong 13 \times 10^{-6}$ sec. For the coupled ZPR-V experiment,[62] only ~25% of the reactivity was due to fast fissions and $\ell_p \cong 39 \times 10^{-6}$ sec.

XVII. TEMPERATURE EFFECTS ON REACTIVITY-SODIUM VOID EFFECT

In thermal reactors increase in temperature, due to increase in fission density, primarily affects reactivity by two mechanisms. One is the decreased density of the fuel and moderator due to thermal expansion upon heating; the temperature increase in the fuel is transmitted to the moderator. The other is the increased moderator temperature, that causes a shift in the quasi-Maxwellian distribution of thermalized neutrons toward slightly higher energies. The first effect results in reactivity change through change in leakage and moderating properties. The second effect causes reactivity change because the absorption cross section in the thermal-energy region generally decrease with increased energy of the incident neturons. The increase in diffusion length then results in increased leakage.

For the case of a large graphite-moderated reactor, a value of -2.6×10^{-5} $(\Delta k/k)/°C$ has been given[1] for the spectral shift effect and of about -2.8×10^{-5} $\Delta k/k/°C$ for the volume-density effect. The later consists of -0.29×10^{-5} $\Delta k/k/°C$ due to density decrease assuming constant volume and of $+0.095 \times 10^{-5}$ $\Delta k/k°C$ due to the accompanying increase in volume due to core leakage.

Density-volume temperature effects also exist in fast systems, but they are often smaller than in thermal systems. The numerous possible expansions and density changes which comprise the overall effect are frequently individually small and difficult to estimate because of the strong dependence upon the particular structural characteristics.

The spectral shift effect is negligible in fast reactors because the neutron spectra are high in energy, so that the effects of lattice vibrations in altering the spectra are negligible.

Lack of the spectral shift effect together with frequently small volume-density effects has necessitated detailed considerations of otherwise numerous small temperature-reactivity effects.

McCarthy[64] gives the following breakdown of the isothermal temperature coefficients (in $\Delta k/k/°C$) for various density-volume effects in the core and blanket of the Fermi Fast Breeder Reactor:

Core:

(a) Axial fuel expansion: -2.5×10^{-6}
(b) Radial fuel expansion (sodium expulsion): -0.6×10^{-6}
(c) Density change of coolant and of subassembly material: -7.1×10^{-6}
(d) Structural expansion: -6.0×10^{-6}

Blanket:

(e) Density change of coolant and of subassembly material: -3.3×10^{-6}
(f) Growth of uranium: -0.5×10^{-6}
(g) Structural expansion: -0.6×10^{-6}

An important contributor to the volume-density effect in fast, sodium-cooled reactors is the reactivity change resulting from decrease in sodium coolant brought about by density decrease with temperature or possibly by accidental sodium expulsion. An overall decrease in mean sodium density in the system can also occur by expansions of fuel rods, which causes a displacement of the sodium. This effect is referred to as the sodium-void reactivity effect. If reactivity increase accompanies sodium loss, the sodium-void coefficient is considered positive; otherwise it is negative. This quantity is receiving much attention because of the possibility in some large fast reactors of having a potentially dangerous positive sodium-void effect.(65)

The sodium-void effect essentially consists of two effects. One is the increased leakage which accompanies the decreased fraction of sodium volume. The magnitude of this effect diminishes with increased core dimensions. The second effect is due to the shift in the fast neutron flux spectrum toward higher energies, resulting from the decreased inelastic and elastic moderation due to loss of some or all of the sodium. The resulting harder fast reactor spectrum tends to increase fertile fission, thereby adding reactivity. The spectral shift can also increase reactivity because the ratio of fissile fission to core absorptions may be greater. Such can be the case, for example, in plutonium-fueled cores for which the fission cross section of plutonium is reasonably constant whereas the core absorption decreases with increasing energies. For U^{235}- or U^{233}-fueled systems this is less likely because energy dependencies of fission and capture properties are closer.

Yiftah and Okrent,(9) using a 16-group cross-section set, calculated that at a core size of about 3500 liters the sodium-void effect becomes positive for the particular Pu^{239} oxide system studied. Examples of the sodium-void curves obtained by them are shown in Fig. 14, where the reactivity change is expressed in terms of $\delta M_c/M_c$, the fractional increment in critical mass which would produce the same reactivity effect as the removal of the sodium.

Calculations of sodium-void effects by the simple expediency of decreasing homogeneously the sodium content in a multigroup analysis consisting of, for example, 16 groups can, of course, only be considered as indicative. Spatial distributions of the sodium voids, effects of scattering resonances of the core materials, and effects of absorption resonances need also be considered. The composite resonances of the various core materials may affect the self-shieldings differently, depending upon amount of sodium. Bhide and Hummel,(66) for example, have re-calculated by means of the

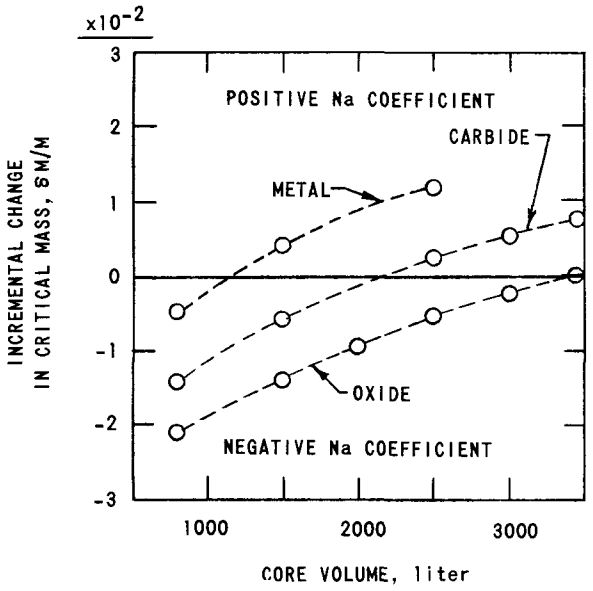

Fig. 14. Reactivity Change Effected by Removal of 40% of Sodium from Plutonium Metal, Plutonium Oxide, and Plutonium Carbide-fueled Cores with Steel Structure (Composite Curves from Ref. 9)

ELMOE program the previously referred-to plutonium oxide-fueled system by taking into account the effect of the scattering resonances. They noted that this lowered the value of the calculated core size at which the sodium-void effect became positive to 2500 liters.

Sodium-void effects may be made more negative (or less positive) by enhancing the reactivity effect of neutron leakage due to sodium loss and by diminishing the reactivity effect of spectral hardening.(65,67-70) Thus, compositions having smaller volume fractions of materials other than sodium should have greater overall transport cross-section decrease with loss of sodium. Enhancement of neutron leakage with loss of sodium by choice of suitable core shapes also might be helpful. Reduction in the amount of fertile material in the core should be helpful by reducing the positive spectral shift effect through decrease of the fast fission contribution of the fertile material. Decrease of structural materials or use of structural materials with very small fast absorption cross sections and/or with energy variations which do not rapidly decrease with increasing energy should also diminish the spectral shift effect.

Currently the sodium-void effect and its relation to other reactor considerations (such as control, breeding, safety, power, and economics) are not sufficiently well understood. The present status of the sodium-void problem and, in addition, the subsequently to be discussed Doppler problem are documented in papers recently presented(70) by numerous investigators.

XVIII. DOPPLER EFFECT

Another reactivity-temperature effect which is receiving considerable attention is the Doppler effect in fast reactors. The energy dependence of the cross sections of the fissile and fertile isotopes have a profuse resonance structure beginning at near thermal energies and continuing well into the spectral region of fast reactors. These give rise to the Doppler effect, which results from the temperature broadening of the resonances coupled with the fact that the neutron flux at a resonance is highly self-shielded. Resonance broadening increase the overall reaction rates by increasing the cross sections in the wings of the resonances.

For small, highly concentrated, fast systems the Doppler effect is generally very small. The neutron spectra are at very high energies. Capture and fission resonances in both fuel and fertile isotopes are highly overlapping, so that temperature broadening does not modify greatly the reaction rates. The neutron energies of most importance to Doppler effects are ~0.1 MeV in these cases.[71] The effect arises primarily from fluctuations in resonance strengths and spacings.

As systems become larger, density-volume effects diminish and the importance of the Doppler effect increases. The lowered spectral distribution then places some neutrons also in the energy region of separated, but not necessarily experimentally resolved, resonances. In this composition region the question of whether or not the quantity of resonance capturing fertile material relative to resonance capture and resonance fissioning fuel material is sufficient to obtain a nonpositive Doppler effect is important.

With still larger systems, especially those containing moderating elements such as carbon or oxygen present in carbide and oxide fuel and fertile materials, the spectra become sufficiently low in energy that part of the spectra lie within the energy regions of resolved resonances. In systems of this size and composition range, it appears most important that a system have a reasonably large negative Doppler effect to insure a prompt-acting reactivity decrease with temperature increase. For example, in the relatively small, hard spectrum, EBR-II, the much larger and overall negative expansion effects of fuel, coolant, and structure override the small but positive calculated value of $\sim +0.4 \times 10^{-6}\ \Delta k/°C$ for the Doppler coefficient.[72] In contrast, a softer-spectrum, low-enrichment, large fast system might have a value of $\sim -10 \times 10^{-6}\ \Delta k/°C$ for the Doppler coefficient.[73] Relatively large negative Doppler effects may in such large systems be most important to compensate for very small expansion and leakage effects, and in some cases to counteract possible positive sodium-void effects. In addition, the possibility of inconsistent expansion in ceramics due to cracking exists. It may be mentioned that power Doppler effects are greater with ceramics because of the smaller heat transfers and capacities.

In any case, insofar as a multigroup Doppler-effect analysis is concerned, the problem is that of obtaining suitable effective group cross sections as a function of temperature such that the reaction rates of the effective cross section times the flux obtained with these effective cross sections result in the correct reaction rates as obtainable from a very detailed fine group analysis. A detailed report on the theoretical and calculational aspects of Doppler effect in fast reactors is given by Nicholson.[74] A general review, of both experiment and analysis, is that of Graves.[75]

Recall that the Doppler-broadened single-level Breit-Wigner formula for process x is:[27,71]

$$\sigma_x(E, T) = \sigma_0 (\Gamma_x/\Gamma)\, \psi(q, \xi),$$

where

$$\psi(q, \xi) = \frac{\xi}{\sqrt{4\pi}} \int_{-\infty}^{+\infty} \frac{\exp\left[-\frac{\xi^2}{4}(q - y)^2\right]}{1 + y^2}\, dy$$

is an obtainable tabulated function and where

$$\sigma_0 = 4\pi \lambda\!\!\!^{-2} g\, \Gamma_n/\Gamma.$$

The parameters are

$$\lambda\!\!\!^{-2} = \hbar^2/\sqrt{2\mu E},$$

where μ is the reduced mass and E is the neutron energy in the laboratory system,

$$g = (2J + 1)/2(2I + 1),$$

where J is the spin of the compound nucleus and I is the spin of the target nucleus,

$$q = (E - E_r)\Big/\frac{1}{2}\Gamma,$$

and

$$\xi = \Gamma/\Delta,$$

where

$$\Delta = \sqrt{4EkT/A}$$

is the Doppler width.

The integral over a resonance for process x is

$$\int_{-\infty}^{+\infty} \sigma_x(E,T)dE = 2\pi^2 g \lambda\!\!\!^{-2} \frac{\Gamma_n \Gamma_x}{\Gamma}.$$

For an energy interval ΔE about E large compared to resonance widths and containing more than one resonance, the average cross section for the resonance process is

$$\overline{\sigma}_{x,E} \cong \frac{1}{\Delta E} \sum_{\substack{\text{resonances} \\ \text{in } \Delta E}} \left(2\pi^2 g \lambda\!\!\!^{-2} \frac{\Gamma_n \Gamma_x}{\Gamma}\right)_{\text{at } E_R},$$

because each resonance contribution is essentially from a small energy interval about E_R. If average resonance spacings $\overline{S}$ and average resonance parameters are used, the formula becomes

$$\overline{\sigma}_{x,E} \cong \left(\frac{1}{\overline{S}}\right) 2\pi^2 \lambda\!\!\!^{-2} \left(\frac{\overline{g\Gamma_n \Gamma_\gamma}}{\Gamma}\right),$$

where the number of resonances,

$$n = \frac{\Delta E}{\overline{S}},$$

and E lies within ΔE. The analogous expression for the compound nucleus is

$$\overline{\sigma}_E \cong (1/\overline{S})\, 2\pi^2 \lambda\!\!\!^{-2}\, (\overline{g\Gamma_n}).$$

In the discussion of flux depletion at resonances, however, it was noted that

$$\phi \sim 1/E\,\sigma(E)$$

at sufficient distances from sources if we may assume constant collision density per unit lethargy. Also, if only a small region ΔE about E is considered, $\phi \sim 1/\sigma(E)$ in ΔE, i.e., $\phi\sigma$ is approximately constant. Then the effective cross section, in ΔE, for resonance process x is

$$\sigma_{x,E}^{eff} \cong \frac{\int_{\Delta E} \frac{\sigma_x}{\sigma}\, dE}{\int_{\Delta E} \frac{dE}{\sigma}} \equiv \frac{\overline{\left(\frac{\sigma_x}{\sigma}\right)}_{\Delta E}}{\overline{\left(\frac{1}{\sigma}\right)}_{\Delta E}},$$

and

$$\phi_E^{eff} = \frac{\int_{\Delta E} \phi(E) dE}{\Delta E} \cong \frac{\int_{\Delta E} \frac{dE}{\sigma}}{\Delta E}.$$

The total cross section is

$$\sigma = \sigma_a + \sigma_s,$$

where σ_a refers to absorption processes and σ_s to scattering processes. The total cross section is often expressed as

$$\sigma = \sigma_0 \psi + \sigma_{nonres},$$

where σ_{nonres} includes the scattering and nonresonant absorption processes. The ratio σ_{nonres}/σ_0, referred to as β, is a frequently used parameter in Doppler effect analyses.(74,75) For example, $\overline{(\sigma_x/\sigma)}_{\Delta E}$ may be expressed as

$$\frac{\Gamma_x}{\Gamma} \int_{\Delta E} \frac{\psi}{\psi + \beta}\, dE.$$

The latter is of the form of the function

$$J(\xi, \beta) = \int_0^{\infty} \frac{\psi}{\psi + \beta}\, dq$$

used in calculations of effective resonance integrals. The self-shielding factor is

$$f = \frac{\sigma_{x,E}^{eff}}{\bar{\sigma}_{x,E}} = \frac{\overline{\left(\frac{\sigma_x}{\sigma}\right)} \Big/ \overline{\left(\frac{1}{\sigma}\right)}}{(\bar{\sigma}_x)}.$$

In this introductory presentation only the treatment of the resonance terms will be discussed. In any complete analyses interference terms between resonance and potential scattering must also be considered.

For the case of resolved resonances these quantities are, of course, related to the effective resonance integrals. These integrals have been based upon the narrow resonance (NR) or narrow resonance infinite absorber (NRIA) assumptions;[76] that is, the average energy loss by elastic collision exceeds the practical width of the resonance, as is usually the case for the higher-energy resolved resonances. At the still lower-lying resonances where the average energy loss may be smaller than the practical width, the NRIA method treats the absorber atoms as infinite in mass. Tables[77] and codes[78] for calculations of Doppler-broadened effective resonance integrals exist.

For unresolved but separated resonances, the NR approximation is again used. The assumption of constant total collision over a resonance is valid for either the narrow well-separated cases or for the narrow closely spaced cases having spacing small compared with the energy loss. The statistical distribution of neutron widths given by Porter and Thomas,[79]

$$P(y)\,dy = \frac{1}{\sqrt{2\pi}} \frac{e^{-y/2}}{\sqrt{y}}\,dy,$$

where

$$y = \Gamma_n/\overline{\Gamma}_n$$

and $\overline{\Gamma}_n$ is the average reduced neutron width. The radiation width and the average level spacing are taken to be constants. For the fission widths the value of the parameter a in the chi-squared distribution,

$$P(y,a) = \frac{\left(\frac{a}{2}\right)}{\Gamma\left(\frac{a}{2}\right)} \left(\frac{a}{2}\,y\right)^{\frac{a}{2}-1} e^{-\frac{a}{2}y},$$

is not certain. Values of 2 and 3 are used (a = 1 for neutron widths).[75]

The region of strong overlapping is also treated by statistical methods.[71,74,75,80] Because of the large energy loss per inelastic collision, a process which is important at these higher energies, compared with the smaller spacing of the levels, the assumption of a constant total collision over any energy interval ΔE containing the resonances is again assumed. Then $\phi(E)\,\sigma(E)$ is approximately constant and

$$\sigma_{x,E}^{eff} = \frac{\int_{\Delta E} \frac{\sigma_x(E)}{\sigma(E)}\, dE}{\int_{\Delta E} \frac{dE}{\sigma(E)}}$$

as previously. Because of the strong overlapping of the many resonances, however, $\sigma(E)$ may be treated as a fairly smooth function with superimposed fluctuations. (Doppler broadening, furthermore, will reduce further these small fluctuations.) For example, widths are ~10 eV and mean spacings ~0.8 eV. Thus

$$\frac{\sigma - \bar{\sigma}}{\bar{\sigma}} << 1,$$

so that

$$\frac{1}{\sigma(E)} = \frac{1}{\bar{\sigma} + [\sigma(E) - \bar{\sigma}]} \cong \frac{1}{\bar{\sigma}} \left[1 - \left(\frac{\sigma(E) - \bar{\sigma}}{\bar{\sigma}}\right)\right]$$

and

$$\left(\frac{1}{\sigma}\right) \cong \frac{1}{\bar{\sigma}}.$$

The effective cross section in ΔE for process x is then expressible in the form

$$\sigma_{x,E}^{eff} = \frac{\int_{\Delta E} \frac{\sigma_x(E)}{\sigma(E)}\, dE}{\int_{\Delta E} \frac{dE}{\sigma(E)}} \cong \bar{\sigma}_x - \left(\frac{\overline{\sigma_x \sigma} - \bar{\sigma}_x \bar{\sigma}}{\bar{\sigma}}\right),$$

where only $\overline{\sigma_x \sigma}$ is a temperature-dependent term; other terms are unweighted and temperature-independent quantities.

Because of resonance overlap it is necessary to use a distribution for the level spacings in addition to the average resonance widths and width distributions.

It may be noted[73] that the resolved region in, for example, the fertile U^{238} isotope is about from 5 to 1,000 eV. The unresolved but well-separated region is about from 1 to 9 keV. In contrast, for the fissionable Pu^{239} isotope the resolved region extends only to about 60 eV.

In concluding this limited presentation, the possible interplay of the sodium-void effect and Doppler effect should be mentioned. For example, an excursion with loss of sodium may result in reduction of Doppler effect through shift of flux distribution toward higher energies at which the Doppler effect is less negative.

In many fast zero-power facilities the fuel and fertile materials are not homogenized, but are, instead, separate pieces. The possibility of fuel temperatures exceeding fertile temperatures might result in a positive or, at least, less negative Doppler coefficient than in the homogenized case.

Last, but not least, is the fast reactor melt-down hazard.(81) Because of the large fissionable material inventory, an excursion which would lead to fuel melting conceivably might produce a highly supercritical configuration.

REFERENCES

1. S. Glasstone and M. C. Edlund, The Elements of Nuclear Reactor Theory, Van Nostrand Co., Inc., Princeton (1952).
2. L. Cranberg et al., Fission Neutron Spectrum of U^{235}, Phys. Rev., 103, 662 (1956).
3. A. B. Smith et al., Precise Determination of the U^{233} Fission Neutron Spectrum, Phys. Rev., 114, 1351 (1959).
4. D. Meneghetti, H. H. Hummel, and W. B. Loewenstein, Ten-group Calculated Equilibrium Neutron Spectrum and Diffusion Length in Natural Uranium, Nuc. Sci. and Eng., 3, No. 2, 151 (1958).
5. D. Okrent, R. Avery, and H. H. Hummel, A Survey of the Theoretical and Experimental Aspects of Fast Reactor Physics, Proc. UN Intnl. Conf. on Peaceful Uses of Atomic Energy, Geneva, Switzerland, 5, 347 (1955).
6. D. J. Hughes, New "World-Average" Thermal Cross Sections, Nucleonics, 17(11) (Nov 1959).
7. G. J. Safford and W. W. Havens, Jr., Fission Parameters for U^{235}, Nucleonics, 17(11) (Nov 1959).
8. Reactor Physics Constants, ANL-5800 (Second Edition, July 1963).
9. S. Yiftah and D. Okrent, Some Physics Calculations on the Performance of Large Fast Breeder Power Reactors, ANL-6212 (1960).
10. B. I. Spinrad, On the Definition of Breeding, ANL-6122 (1959).
11. A. B. Smith, A Critical Summary of Microscopic Fast-neutron Interactions with Reactor Structural, Fissile and Fertile Materials, Proc. of Seminar on Physics of Fast and Intermediate Reactors, IAEA, Paper SM-18/76, Vienna (1961).
12. L. J. Koch and H. C. Paxton, Fast Reactors, Vol. 9, p. 437, Annual Rev. Nuclear Science (1959).
13. D. J. Hughes and R. B. Schwartz, Neutron Cross Sections, 2nd Edition, BNL-325 (1958).
14. S. Glasstone, Principles of Nuclear Reactor Engineering, Van Nostrand, Princeton (1955).
15. R. G. Palmer and A. Platt, Fast Reactors, Temple Press, London (1961).
16. A. Amorosi and J. G. Yevick, An Appraisal of the Enrico Fermi Reactor, Proc. 2nd UN Intnl. Conf. on Peaceful Uses of Atomic Energy, Geneva, Switzerland, 9, 358 (1958).

17. H. A. Bethe, Fast Breeders Are Essential to Future Atomic Power, Nucleonics, 15, 61 (1957).

18. F. W. Thalgott, et al., Stability Studies on EBR-I, Proc. 2nd UN Intnl. Conf. on Peaceful Uses of Atomic Energy, Geneva, Switzerland, 12, 242 (1958).

19. R. L. Murray, Nuclear Reactor Physics, Prentice Hall, Inc., Englewood Cliffs, N. J. (1957).

20. R. Ehrlich and H. Hurwitz, Jr., Multigroup Methods for Neutron Diffusion Problems, Nucleonics (Feb 1954).

21. J. B. Scarborough, Numerical Mathematical Analysis, 2nd Ed., Johns Hopkins Press, Baltimore (1950).

22. P. F. Zweifel and G. L. Ball, Group Cross Sections for Fast Reactors, Proc. of Seminar on Physics of Fast and Intermediate Reactors, Paper SM-18/65, Vienna (1962).

23. S. Yiftah, D. Okrent, and P. A. Moldauer, Fast Reactor Cross Section, Pergamon Press, New York (1960).

24. A. I. Novozhilov and S. B. Shikhov, A Method of Averaging Nuclear Constants in Fast Reactor Calculations Taking Into Account Neutron Weighting, Atomnaya Energiya 8, translation by N. Kemmer, Reactor Science and Technology, 16, 137 (1962).

25. D. S. Selengut, Variational Analysis of Multi-dimensional Systems, Trans. Amer. Nucl. Soc., 2, No. 1, p. 58 (1959).

26. G. D. Joanou and J. S. Dudek, GAM-I: A Consistent P_1 Multigroup Code for the Calculation of Fast Neutron Spectra and Multigroup Constants, GA-1850 (1961).

27. A. M. Weinberg and E. P. Wigner, The Physics Theory of Neutron Chain Reactors, The University of Chicago Press, Chicago (1958).

28. E. D. Pendlebury and L. H. Underhill, The Validity of the Transport Approximation in Critical-size and Reactivity Calculations, Proc. of Seminar on Phys. of Fast and Intermediate Reactors, Paper SM 18/21, Vienna (1962).

29. G. D. Joanou and A. H. Kazi, The Validity of the Transport Approximation in Fast-Reactor Calculations, Trans. Am. Nucl. Soc., 6, No. 1, 17 (1963).

30. H. Hummel and A. Rago, An Accurate Treatment of Resonance Scattering in Light Elements in Fast Reactors, Proc. of Seminar on Phys. of Fast and Intermediate Reactors, Paper SM-18/45, Vienna (1962).

31. Z. Kopal, Numerical Analysis, J. Wiley and Sons, Inc., New York (1955).

32. R. D. Richtmyer, Difference Methods for Initial-value Problems, Interscience Publishers, New York (1957).

33. H. Margenau and G. M. Murphy, The Mathematics of Physics and Chemistry, Van Nostrand Co., New York (1943).

34. L. A. Hageman and J. T. Mandel, RANCH - An IBM-704 Program Used to Solve the One-dimensional Single-energy Neutron Transport Equation with Anisotropic Scattering, WAPD-TM-268 (1961).

35. B. G. Carlson, Solution of the Transport Equation by S_N Approximation, LA-1891 (1955).

36. B. Carlson, C. Lee, and J. Worlton, The DSN and TDC Neutron Transport Codes, LAMS-2346 (1960).

37. B. G. Carlson and G. I. Bell, Solution of the Transport Equation by the S_N Method, Proc. of the 2nd UN Intnl. Conf. on Peaceful Uses of Atomic Energy, Geneva, Switzerland, 16, 535 (1958).

38. R. M. Kiehn, Some Applications of the S_N Method, Nuclear Sci. and Eng., 4, 166 (1958).

39. B. Carlson, Numerical Solution of Transient and Steady State Neutron Transport Problems, LA-2260 (1959).

40. H. Hurwitz, Jr. and P. F. Zweifel, Slowing Down of Neutrons by Hydrogeneous Moderators, J. Appl. Phys. 26, 923 (1955).

41. W. B. Loewenstein and D. Meneghetti, Integral Physics Data for Fast-reactor Design, Proc. Seminar Phys. of Fast and Intermediate Reactors, Paper SM-18/77, Vienna (1962).

42. C. G. Chezem, A Uranium Exponential Experiment, Nuclear Sci. and Eng., 8, 652 (1960).

43. A. I. Leipunsky et al., Studies in the Physics of Fast Neutron Reactors, Proc. 2nd UN Intnl. Conf. on Peaceful Uses of Atomic Energy, Geneva, Switzerland, 12, 3 (1958).

44. J. E. R. Holmes et al., Experimental Studies on Fast Neutron Reactors at AERE, Proc. Intnl. Conf. on Peaceful Uses of Atomic Energy, Geneva, Switzerland, 5, 331 (1955).

45. J. E. Brolley et al., Neutron Multiplication in a Mass of Uranium Metal, The University of Chicago Metallurgical Project Report CF-1627 (1944).

46. F. C. Beyer et al., The Fast Exponential Experiment, Proc. UN Intnl. Conf. on Peaceful Uses of Atomic Energy, Geneva, Switzerland, 5, 342 (1955).

47. D. Meneghetti, H. H. Hummel, and W. B. Loewenstein, Equilibrium Spectrum and Diffusion Length in Natural Uranium, Nuclear Sci. and Eng., 3, 772 (1958).

48. D. Meneghetti, Recent Advances and Problems in Theoretical Analyses of ZPR-III Fast Critical Assemblies, Proc. Seminar on Physics of Fast and Intermediate Reactors, Paper SM-18/37, Vienna (1962).

49. H. Soodak, Reactor Handbook, Volume III, Part A, Physics, Interscience Publishers, New York (1962).

50. J. K. Long et al., Experimental Results on Large Dilute Fast Critical Systems with Metallic and Ceramic Fuels, Proc. Seminar on Physics of Fast and Intermediate Reactors, Paper SM-18/48, Vienna (1962).

51. G. R. Keepin, T. F. Wimett, and R. K. Zeigler, Delayed Neutrons from Fissionable Isotopes of Uranium, Plutonium, and Thorium, LA-2118 (1957).

52. G. R. Keepin, T. F Wimett, and R. K. Zeigler, Delayed Neutrons from Fissionable Isotopes of Uranium, Plutonium, and Thorium, Phys. Rev., 107, 1044 (1957).

53. G. R. Keepin, Neutron Data for Reactor Kinetics, Nucleonics, 20, 150 (1962).

54. R. Batchelor and H. R. McK. Hyder, The Energy of Delayed Neutrons from Fission, J. Nuclear Energy, 3, 7 (1956).

55. J. K. Long et al., Fast Neutron Power Reactor Studies with ZPR-III, Proc. 2nd UN Intnl. Conf. on Peaceful Uses of Atomic Energy, Geneva, Switzerland, 12, 119 (1958).

56. G. S. Brunson et al., Measuring the Prompt Period of a Reactor, Nucleonics, 15, 11 (1957).

57. J. Codd, M. F. James, and J. E. Mann, Some Physics Aspects of Cermet and Ceramic Fast Systems, Proc. Seminar on Physics of Fast and Intermediate Reactors, Paper SM-18/14, Vienna (1962).

58. W. B. Loewenstein and G. W. Main, The Influence of Core Shape on Fast Reactor Criticality, Trans. of Amer. Nucl. Soc., 5, No. 1, 61 (1962).

59. W. B. Loewenstein and G. W. Main, Fast Reactor Shape Factors and Shape-dependent Variables, ANL-6403 (1961).

60. R. Avery, Theory of Coupled Reactors, Proc. 2nd UN Intnl. Conf. on Peaceful Uses of Atomic Energy, Geneva, Switzerland, 12, 182 (1958).

61. R. Avery et al., Coupled Fast-thermal Power Breeder Critical Experiment, ibid., 12, 151 (1958).

62. H. H. Hummel et al., Experimental and Theoretical Studies of the Coupled Fast-thermal System ZPR-V, ibid., 12, 166 (1958).

63. H. A. Morewitz and S. G. Carpenter, The Epithermal Critical Experiments, Proc. Seminar on Physics of Fast and Intermediate Reactors, Paper SM-18/60, Vienna (1962).

64. W. J. McCarthy, Jr., et al., Studies of Nuclear Accidents in Fast Power Reactors, Proc. 2nd UN Intnl. Conf. on Peaceful Uses of Atomic Energy, Geneva, Switzerland, 12, 207 (1958).

65. J. B. Nims and P. F. Zweifel, Sodium Temperature Coefficients in Fast Reactors, Trans. Amer. Nuclear Soc., 2, 172 (1959).

66. M. G. Bhide and H. H. Hummel, Reactivity Coefficients of Sodium in Some Large Fast Reactors, Proc. Seminar on Phys. of Fast and Intermediate Reactors, Paper SM-18/72, Vienna (1962).

67. H. H. Hummel et al., Using Plutonium in Fast Reactors, Nucleonics, 21, No. 1, 43 (1963).

68. P. Greebler, B. A. Hutchens, and J. R. Sueoka, Calculation of Doppler Coefficient and Other Safety Parameters for a Large Fast Oxide Reactor, GEAP-3646 (1961).

69. K. M. Horst and B. A. Hutchens, Comparative Study of PuC-UC and PuO_2-UO_2 as a Fast Reactor Fuel, GEAP-3880 (1962).

70. Proceedings of the Conference on Breeding, Economics, and Safety in Large Fast Power Reactors, October 7-10 1963, ANL-6792 (Dec 1963).

71. G. Goerzel, An Estimate of Doppler Effect in Intermediate and Fast Neutron Reactors, Proc. Intnl. Conf. on Peaceful Uses of Atomic Energy, Geneva, Switzerland, 5, 472 (1955).

72. W. B. Loewenstein, The Physics Design of EBR-II, Proc. Seminar on Phys. of Fast and Intermediate Reactors, Paper SM-18/39, Vienna (1962).

73. P. Greebler and B. A. Hutchins, The Doppler Effect in a Large Fast Oxide Reactor - Its Calculation and Significance for Reactor Safety, Proc. Seminar on Physics of Fast and Intermediate Reactors, Paper SM-18/59, Vienna (1962).

74. R. B. Nicholson, The Doppler Effect in Fast Neutron Reactors, APDA-139 (1960).

75. C. C. Graves, A Review of Analytical and Experimental Work Pertinent to the Doppler Effect in Fast Reactors, UNC-5034 (1962).

76. L. Dresner, Resonance Absorption in Nuclear Reactors, Pergamon Press, New York (1960).

77. F. T. Adler, G. W. Hinman, and L. W. Nordheim, The Quantitative Evaluation of Resonance Integrals, Proc. of 2nd UN Intnl. Conf. on Peaceful Uses of Atomic Energy, Geneva, Switzerland, 16, 155 (1958).

78. F. L. Fillmore, ARES - A Resonance Integral Code, Trans. Am. Nucl. Soc., 5, 57 (1962).

79. C. E. Porter and R. G. Thomas, Fluctuations of Nuclear Reaction Widths, Phys. Rev. 104, 483 (1956).

80. A. M. Lane, J. E. Lynn, and J. S. Story, An Estimation of the Doppler Effect in Fast Neutron Reactors, AERE T/M 137 (1956).

81. D. Okrent, A Review of the Nuclear Aspects of Fast-Reactor Safety, Proc. of Seminar on Physics of Fast and Intermediate Reactors, Paper SM-18/78, Vienna (1962).